DISCLAIMER

This report was prepared as an account of work sponsored by an agency of the United States Government. Neither the United States Government nor any agency thereof, nor any of their employees, makes any warranty, express or implied, or assumes any legal liability or responsibility for the accuracy, completeness, or usefulness of any information, apparatus, product, or process disclosed, or represents that its use would not infringe privately owned rights. Reference herein to any specific commercial product, process, or service by trade name, trademark, manufacturer, or otherwise does not necessarily constitute or imply its endorsement, recommendation, or favoring by the United States Government or any agency thereof. The views and opinions of authors expressed herein do not necessarily state or reflect those of the United States Government or any agency thereof. Reference herein to any social initiative (including but not limited to Diversity, Equity, and Inclusion (DEI); Community Benefits Plans (CBP); Justice 40; etc.) is made by the Author independent of any current requirement by the United States Government and does not constitute or imply endorsement, recommendation, or support by the United States Government or any agency thereof.

Cover Page

***a.** Federal Agency*	Department of Energy	
***b.** Award Number*	DE-EE0008836	
***c.** Project Title*	Performance and Durability Investigation of Thin, Low Crossover Proton Exchange Membranes for Water Electrolyzers	
***d.** Recipient Organization*	The Chemours Company FC, LLC	
***e.** Project Period*	*Start*: 03/01/20	*End*: 12/31/23
***f.** Principal Investigator (PI)*	Andrew M. Park Senior Principal Engineer Andrew.park1@chemours.com 302-773-6627	
***g.** Business Contact (BC)*	Tim Hopkins Director, Chemours Discovery Hub Timothy.e.hopkins@chemours.com 302-773-6542	
***h.** Teaming Partners*	Los Alamos National Lab (LANL) HydroGEN node partners: National Renewable Energy Lab (NREL) Lawrence Berkeley National Lab (LBNL)	

Acknowledgement: This material is based upon work supported by the U.S. Department of Energy's Office of Energy Efficiency and Renewable Energy (EERE) under the Hydrogen and Fuel Cell Technologies Office (HFTO), Award Number DE-EE0008836.

Executive Summary: In order to unleash America's affordable and reliable energy, one critical technology is the deployment of low cost hydrogen. The Department of Energy's hydrogen shot goal of $1/kg produced H_2 requires significant advances in technology to reduce the cost of hydrogen. One of the most promising technologies for inexpensive hydrogen production is the proton exchange membrane water electrolyzer (PEMWE). PEMWEs convert water to hydrogen and oxygen using electricity. The technology utilizes a proton exchange membrane (PEM) separator at the center of the electrochemical core. At the start of this project, the membranes used and proven durable in this application were extremely thick (up to 250 µm). This represented a significant efficiency penalty (higher cost) toward converting electricity into hydrogen. While thinner membranes were available and used in other applications, simply employing them instead of the thick incumbents would increase the rate of hydrogen crossover across the membrane, leading to unsafe mixtures of hydrogen in the oxygen stream (H_2 in O_2).

The goal of this project was to fabricate and study the performance and durability implications of thin, mechanically reinforced membranes containing gas recombination catalysts (GRCs) for advanced PEMWE systems. The thinner membranes, optimized for a PEMWE environment, dramatically reduced the proton transport resistance across the membrane, improving the overall efficiency of the PEMWE system. At the same time, the GRC technology was deployed to recombine crossover hydrogen from the cathode with oxygen from the anode to form water within the membrane. This reaction mitigated the buildup of hydrogen in the oxygen stream, ensuring safe operation of the PEMWE system. Capabilities to measure the gas crossover in both an ex-situ screening cell (LANL) and in operando application testing (NREL) were developed over the course of the project to track membrane progress and quantify deliverables. State of the art (SOA) roll to roll (R2R) manufacturing technologies were leveraged to fabricate the membranes on a commercial scale, where the membrane structure was precisely tuned and GRC distributed within the membrane structure.

The project outcome was a successful PEMWE beginning-of-life membrane demonstration that (1) improved PEMWE efficiency from 60% with benchmark membranes to 72% compared to benchmark membranes, (2) reduced effective gas crossover by a factor of >50x, and (3) was able to be manufactured at pilot scale on Chemours' SOA membrane manufacturing asset for subsequent conversion to a commercial, domestically manufactured product. The project clarified the future work necessary to focus on durability of the membrane's mechanical properties and GRC behavior, and the need for expansion of experimental bandwidth to probe these topics most effectively. The project directly or indirectly supported jobs at Chemours facilities in Fayetteville, NC and Newark, DE and helped lead to the domestic expansion of a membrane manufacturing facility in Elkton, MD. As the only domestic manufacturer of polymers and membranes for the PEMWE industry, the project advanced technology that will enable domestic manufactured membranes for PEMWE to maintain a leading and competitive position in the global market.

Table of Contents:

Background: PEMWE utilized up to an order of magnitude thicker membranes compared to fuel cells because of crossover concerns with a high differential pressure environment. This project sought to investigate GRCs as a solution to high gas crossover in thinner membranes. The concept of a GRC has been disclosed in fuel cell research since the late 1990s and has been discussed for PEMWE membranes in academic literature. GRCs were dispersed in Nafion™ perfluorosulfonic acid (PFSA) dispersion and coated in a roll to roll (R2R) process where the GRCs were deposited in a discrete layer within the PEM near the anode surface. This GRC layer in the membrane reacts hydrogen gas crossing through the membrane with oxygen to form water. The GRC layer within the membrane was studied for its optimum content/placement for reducing hydrogen content in the oxygen stream, and its stability toward migration or dissolution within the membrane during dynamic operation.

While the GRC approach is fundamentally necessary to enable thin membranes in PEMWE, degradation concerns associated with radical species generated by metals contamination and dynamic operation could be exacerbated. Radical species, particularly the hydroxyl radical, may cause irreversible degradation of the PFSA macromolecule, leading to global PEM thinning and decay of its mechanical properties, resulting in eventual system failure. To protect the membrane from these degrading moieties, radical scavengers were dispersed within the PFSA during dispersion manufacturing. These compounds were investigated and developed to increase their effectiveness and reduce migration in PEMWEs.

Project Objectives: The goal of this project was to develop the technology and to fabricate and validate the performance and durability of thin, mechanically reinforced membranes where gas recombination catalysts (GRCs) and potentially radical scavengers were included to reduce gas cross-over and increase durability, respectively, for advanced proton exchange membrane water electrolyzer (PEMWE) systems. State of the art (SOA) roll to roll (R2R) manufacturing technologies were leveraged to fabricate the membranes on a commercial scale, where the placement and loading of the additives were precisely tuned/distributed within the membrane structure. The critical factors for success included (1) integrating/optimizing additives within a thin, reinforced PFSA membrane, (2) understanding the behavior of the additives (i.e. activity, migration, dissolution, and/or retention) within the membrane over a PEMWE-relevant lifetime, and (3) validating membrane performance/durability using application testing (membrane electrode assembly (MEA) operando cells) that are representative of dynamic operation during H2@Scale applications.

The manufacturing and material advancements initially proposed were intended to facilitate PEMWEs to meet defined targets in terms of improved performance, durability, cost, and ease of manufacture. Project specific targets are given below in Table 1. Major improvements included (1) significant reduction in ohmic losses associated a thinner membrane, (2) safe/minimal levels of hydrogen crossover with high differential pressures assured by GRCs, (3) high durability and improved tolerance to Fenton's metals from stable radical scavengers, and (4) major cost reductions and productivity improvements moving from thick extruded films to dispersion-cast, R2R coated membranes. The vision was to enable widespread deployment of high performance, durable PEMWE systems resilient to dynamic operation, enabling renewable penetration on the electrical grid to support the H2@Scale concept.

Table 1: Project Technical Targets

#	Metric	SOA status	Project target	Ultimate target
1	**Membrane resistance [Ω-cm^2]** [a]	0.2 [c]	< 0.05	< 0.025
2	**Membrane in-plane expansion (%)**[b]	20	<10	<5
3	**Membrane tensile strength (MPa)**[b]	25	>40	>45
4	**Gas crossover rate [%H_2 in O_2]** [d]	2.0 [d]	< 2.0	< 0.5
5	**Hydrogen Outlet Pressure [bar]**	30 [e]	30	Up to 950 [e]
6	**Fe(III) tolerance [mg/L]** [f]	10 [f]	>10	>100
7	**GRC Content (mg/cm^2)**	0.02	<0.05	<0.02
8	**Radical scavenger mobility [m^2/Vs]** [h]	2.1×10^{-8} [i]	< 2.1×10^{-8}	< 2.1×10^{-8}
9	**Radical scavenger in PEM after duty cycle/AST [% initial concentration]**	n/a	> 50	> 80
10	**FER during duty cycle/AST [h]** [j]	n/a	TBD	Extrapolated 10-20 years with power cycling
11	**Membrane Cost [$/m^2]**	Nafion™ 1110 [j]	~ Nafion™ XL	< Nafion™ XL [k]
12	**Manufacturing speed [m^2/year]**	Nafion™ 1110	> Nafion™ 1110	> Nafion™ XL

a. *High-frequency resistance in liquid water at 80°C with 1.5V applied potential*
b. *From Nafion Technical Bulletin: N115/117/11101*
c. *From Su et al.2*
d. *From Bessarabov et al.3*
e. *From Hamdan et al.4*
f. *Fluoride emissions during Fenton's test with membrane immersed in 1M H_2O_2 and appropriate concentrations of ppm Fe*
g. *From Gubler et al.5*
h. *Using H_2 pump migration measurement technique in liquid water at 80°C with 2V applied potential, adapted from Baker et al.6*
i. *From Baker et al.6*
j. *Relevant AST/duty cycle established and targets defined in the work scope described in this proposal*
k. *Nafion™ 1100 and XL are the SOA extruded and R2R manufactured membranes, respectively, from Chemours*

This project focused on the development of high performing membranes for PEMWE via R2R manufacturing. These PFSA membranes were mechanically-reinforced, with chemical additives (GRCs and radical scavengers) for improved durability and low cross-over, enabling simultaneous high hydrogen outlet pressures and low proton transport resistance. These advanced membranes were substantially thinner (~25-50 μm) compared to the current SOA electrolysis membranes in use (~250 μm). They incorporated several novel technologies for water electrolysis, including additives for gas recombination (GRCs), low mobility/high activity radical scavengers for durability improvement, and other polymer technologies such as advanced polymer chemistries. All membrane improvements were combined into a commercial-scale prototype produced by R2R manufacturing at a substantially higher throughput and lower cost than the current SOA extrusion methods. At the end of the project, Chemours demonstrated R2R manufacturing of the optimized PEMWE membrane design.

Budget Period 1 (BP1) focused on proving the concept of using thin, reinforced membranes for water electrolyzers without necessarily incurring gas crossover concerns due to GRC layers. Methods and baseline materials were established to verify project progress, and lab-scale membranes were evaluated for success at beginning of life conditions. Budget Period 2 (BP2) expanded on that work by probing the durability implications of the thinner membranes at device relevant operating conditions, as well as understanding the mobility and/or morphological changes associated with the additives. This work is necessary to ensure that any mitigation strategies for crossover or radical scavenging are effective over the course of a PEMWE membrane's lifetime. Budget Period 3 (BP3) incorporated optimized additive and membrane composition into roll to roll manufacturing to demonstrate the commercial relevance of the thin, reinforced PEMWE membrane approach. Also, fundamental understanding to guide further development of membranes in the field was disseminated.

HydroGEN Energy Materials Network (EMN) Consortium resources were leveraged. Close collaboration with HydroGEN labs such as NREL and LBNL included exchange of data and materials as needed to facilitate project success. Specific tasks and a milestone table are provided in Appendix A.

Project Results and Discussion:

1. List of Milestones and End of Project Status

Milestone M1: Define initial electrolysis membrane MEA material sets and ASTs which are capable of providing performance of at least 2 A/cm2 at 1.9 V.

Status: Complete, except for AST component. See Table 9 and discussion on page 31.

Milestone M2: Establish test for gas crossover (H_2 in O_2 content) for electrolyzer MEAs, and acquire baseline crossover/performance for N115/7, NR212-containing MEAs

Status: Complete. See Figure 35

Milestone M3: Manufacture membranes with at least 3 different additives for gas recombination and radical scavenging and evaluate their activity for H2 and O2 recombination/radical scavenging by monitoring H2 in O2 content and FER, respectively, at beginning of life (BoL) targeting 2% H2 in O2 for all current densities between 0.5 and 2 A/cm2 and an FER <0.25 µg/cm2-hr, a factor of 40x lower than NR211 in the DOE fuel cell combined chemical/mechanical AST.

Status: Mostly Complete. See Figures 12 and 24. A capability to measure fluoride emission rate (FER) for PEMWE membranes was not developed in this program due to lack of resources available. It was determined with DOE project management that running PEMWE membranes in accelerated stress tests (ASTs) on fuel cell test stations to acquire an FER was not a good use of FFRDC resources.

Go/No-Go G1: A ≤50 µm thick PFSA-based membrane with gas recombination catalyst layer (GRC PGM maximum loading of 0.1 mg/cm2) demonstrates at least 50% reduction in H2 in O2 (outlet) content (maximum of 2% H2 in O2 for all current densities between 0.5 and 2 A/cm2) compared to membrane with equivalent thickness without GRC layer. Membrane resistance must be <0.07 Ω-cm2 and current density must reach 2 A/cm2 at <1.9V, with all targets to be met in a PEMWE MEA at 60°C and with a differential pressure of 1-10 bar.

Status: Complete. See Figure 39, with supporting details in Figure 34 and its discussion

Milestone M5: Begin AST testing of roll to roll fabricated reinforced membranes; quantify membrane FER to evaluate effect of different radical scavenger composition/loading with target FER <0.1 µg/cm2-hr.

Status: Incomplete. Please see discussion above for Milestone M3 regarding FER and AST testing.

Milestone M6: Manufacture and evaluate series (minimum 5 different samples) of membranes with different thicknesses and GRC layer compositions to determine effect of GRC placement/loading on H2 in O2 content targeting <2% H2 in O2 for all current densities between 0.5 and 2 A/cm2.

Status: Complete. See Figure 38

Milestone M7: *Achieve H_2 in O_2 content of <2% for all current densities between 0.5 and 2 A/cm2 for a membrane with a GRC layer as a function of hydrogen back pressure from 10-30 bar in a PEMWE MEA at 60°C.*

Status: Complete. See Figure 39.

Go/No-go G2: Reinforced roll-to-roll dispersion cast membrane with GRC (<0.075 mg PGM/cm2) and radical scavenging additives demonstrates a H2 in O2 content of <2% for all current densities between 0.5 and 2 A/cm2 where membrane thickness is ≤ 50 µm, membrane resistance is < 0.05 Ω-cm2, and hydrogen backpressure is 30 bar. Voltage in an MEA at 2 A/cm2 must be < 1.9 V and membrane resistance/gas crossover must remain <0.4% H2 in O2 after 500 hr of continuous operation at 60 oC and differential pressure of 30 bar.

Status: Mostly Complete. All targets met except for the last, where membranes tested for 500 hours demonstrated 0.5%-0.6% H_2 in O_2 after ~500 hours of continuous operation at 80°C. Please see page 42 and Figure 42 for discussion.

Milestone M9: Complete evaluation of low EW ionomers in reinforced membrane to determine impact of chemistry on operation temperature, performance, and durability of electrolyzer membrane leading to down-select decision on pursuing low EW ionomers.

Status: Complete. See Figure 33

Milestone M10: Optimize GRC and radical scavenger additives content with a Pt loading of <0.05 mg/cm2 for use in large scale R2R manufacturing of <50 µm membrane:

Status: Complete. See Figure 40.

Milestone M11: Finish AST testing on down-selected material set giving > 10 mg/L Fe(III) tolerance and maintaining > 50% concentration of the radical scavenger in the membrane. Report on retention/mobility of GRC and radical scavengers in water wet PEMWE condition. Report FER from PEMWE-specific AST.

Status: Incomplete. See discussion above for Milestone M3. In addition, iron tolerance testing was not pursued in this project due to personnel turnover at LANL.

Milestone M12: Demonstrate prototype manufacturing of > 100 linear meters of down-selected membrane design on Chemours' R2R manufacturing line with < 0.05 Ω-cm2 membrane resistance, < 1% H2 in O2 content for all current densities in an MEA, > 10 mg/L Fe(III) tolerance, with additive nanoparticle mobility of < 2.1x10-8 m2/Vs, maintaining > 50% concentration in the membrane and improved lifetime after defined duty cycle/AST, with capacity to produce membranes at costs/rates comparable to Nafion™ XL.

Status: Mostly Complete. DOE Project Management agreed that manufacturing 100 linear meters of membrane solely to meet the milestone was unnecessary, and that the capability to manufacture 100 linear meters was sufficient. All other metrics were met, with the exception of those related to capabilities not developed in the project as discussed.

2. Membrane and Additive Component Layer Manufacturing and Performance Evaluation

2.1 Gas Recombination Catalyst (GRC) Layer Development

Several processes were evaluated at Chemours where gas recombination catalysts were incorporated into a membrane. Three overall categories studied to make a membrane include: (A) spraying GRC onto a preformed membrane, (B) sonicating GRC into Nafion™ dispersion, and (C) blending Nafion™ dispersion and a pre-formed GRC nanoparticle dispersion.

Figure 1 below shows initial results with spraying a GRC layer onto Nafion™ NR212 membrane. A Sono-tek instrument was employed to atomize a suspension of GRC in a layer-by-layer deposition method similar to electrode fabrication strategies performed in FC-PAD fuel cell MEAs and also used for GRC layers in the literature7,8.

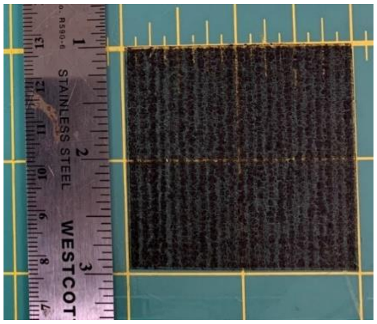

Figure 1. Sprayed GRC layer with Nafion™ overlayer onto an NR212 membrane

Obviously, ridges/mudcracks have formed where the GRC coating is not evenly distributed over the planar area of the membrane. This is common in un-optimized Sono-tek spraying, where the liquid suspension is not adequately evaporated/dried upon contact. Some tuning is required to fabricate a consistent GRC coating. However, the Nafion™ overlayer is easily controlled with the Sono-tek method to a thickness of 2-3 micrometers.

Figure 2 summarizes initial work in Process B where a GRC was added to Nafion™ dispersion via sonication, then coated to form a membrane. Process B1 leverages a pre-sonication step where GRC was dispersed in a mixture of n-propanol/water, then added to Nafion™ dispersion, while Process B2 comprises directly sonicating the GRC in the Nafion™ dispersion. In each case, large GRC agglomerates are observed in scanning electron microscopy (SEM) micrographs of the formed membranes. GRC is highlighted via elemental mapping.

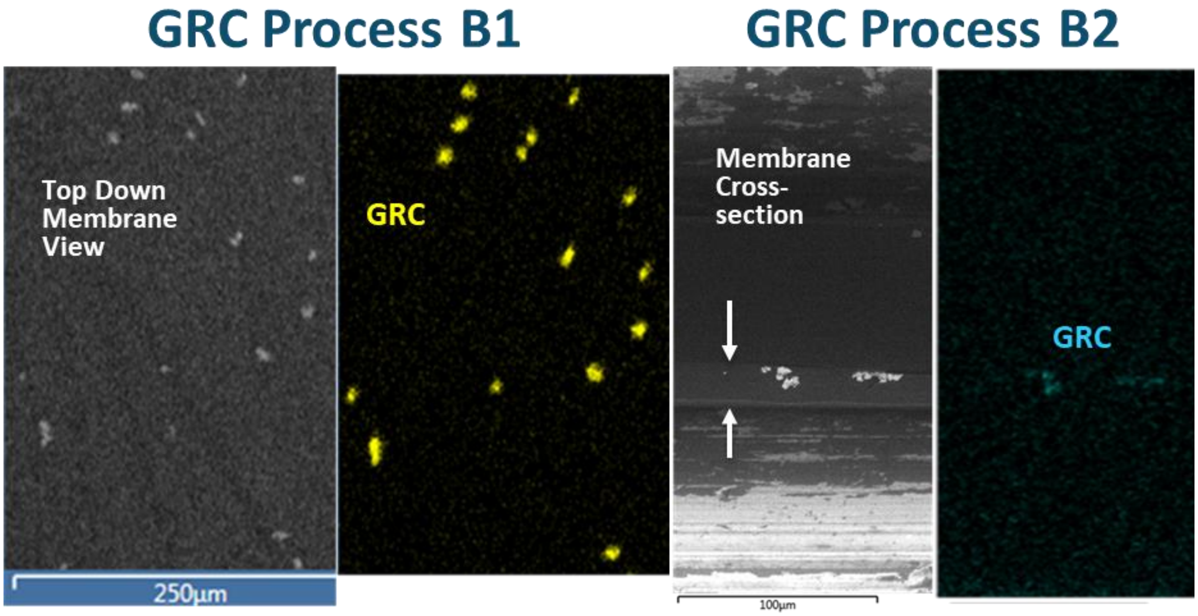

Figure 2. GRC agglomerates in Nafion™ membranes. Please note the first process image is top-down, and the second process image is of a cross section.

Further work involved incorporating multiple GRC dispersions via process C, where nanoparticle solutions were blended into Nafion™ dispersion. Below, Figure 3 shows a back-scatter electron image from an SEM with GRC elemental mapping. A well dispersed GRC is evident. The GRC is contained in a discrete layer within the through-plane Nafion™ membrane thickness. This layer is tunable in terms of concentration, location, and thickness.

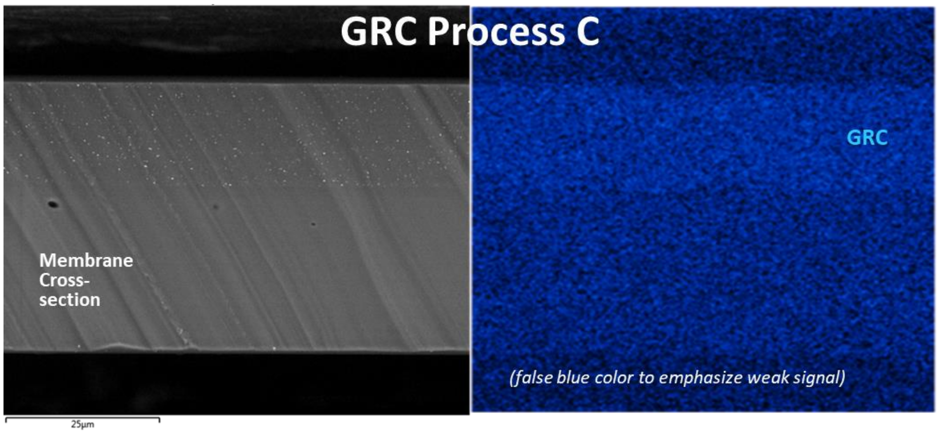

Figure 3. GRC Process C with elemental mapping showing uniform distribution.

Figure 4 contains an optical image of a thin Nafion™ dispersion coating, where the GRC has been incorporated into the membrane via process C. A consistent, gray haze is noted in the membrane coating, evidencing a homogeneous distribution of the GRC material as seen in the corresponding SEM image.

Figure 4. GRC incorporated into custom Nafion™ film

2.2 Membrane Composite Structure Optimization

An initial baseline reinforced membrane candidate was developed with Nafion™ ionomer and expanded polytetrafluoroethylene (ePTFE) reinforcement, represented in Table 2 below as NDP 4006. NDP 4006 was produced on the pilot scale and is compared to commercial Nafion™ membranes. NDP 4006 appears effective at leveraging the inclusion of an ePTFE reinforcement to improve mechanical properties and reduce in plane (x-y) swelling, similar to state-of-the-art thin fuel cell films. The areal resistance is similar to an unreinforced NR212 cast membrane at the same thickness.

Table 2. Baseline and Reinforced Candidate Membrane Parameters

Membrane	Dry Thickness (μm)	Reinforced?	Areal Resistance in 23°C H_2O [mΩ-cm^2]	Ultimate Tensile Strength [MPa]		Liquid H_2O Expansion [%]	
				MD	TD	MD	TD
N117	178	No	217	25	25	13	22
N115	127	No	156	31	28	11	19
NR212	50	No	78	32	32	20	20
NDP 4006	50	Yes	81	43	42	13	8

To improve on the initial reinforced membrane prototype represented by NPD 4006, a series of membranes were evaluated to optimize EW and reinforcement type in the final structure. Table 3 contains the parameters studied. NDP 4006 is represented by the combination of reinforcement A and EW 2. The effect on proton transport resistance was evaluated in a through-plane conductivity test apparatus at 80°C and 95% RH, with results are presented in Figure 5 below.

Table 3. Parameters studied in membrane composition

Reinforcement [g/g]	Equivalent Weight (EW) [g/mol]
Baseline Mass (A)	Low (1)
0.75x Baseline Mass (B)	Moderate (2)

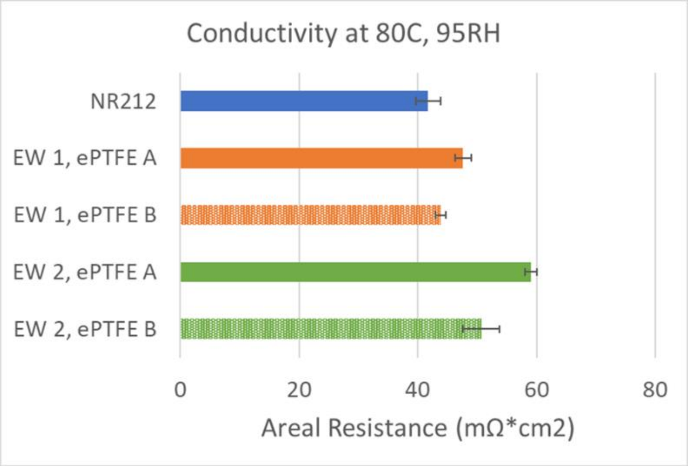

Figure 5. Through plane resistance of membrane prototypes made on pilot scale by Chemours.

It is apparent that EW 1 (where EW 1 < EW 2) is successful in reducing the proton resistance of the membranes, while ePTFE B (at 0.75x the mass of ePTFE) has a similar effect. The effect of reduced proton transport resistance is confirmed in an MEA in Figure 36.

The effect of Nafion™ equivalent weight (EW) and ePTFE reinforcement basis weight was also evaluated for their contributions to composite membrane crossover reduction, utilizing methods described in Section 4. These effects are relevant to the actual amount of hydrogen crossing over the membrane (i.e., energy efficiency), where GRC is a mitigation strategy for hydrogen crossover that does not change the permeation rate of hydrogen. Figure 6 shows the observed data. A parametric study was performed with 4 membranes, where each membrane contained a unique combination of EW and reinforcement. Each membrane was 50 µm in thickness and produced on the Chemours pilot line. See Table 3 for composition information.

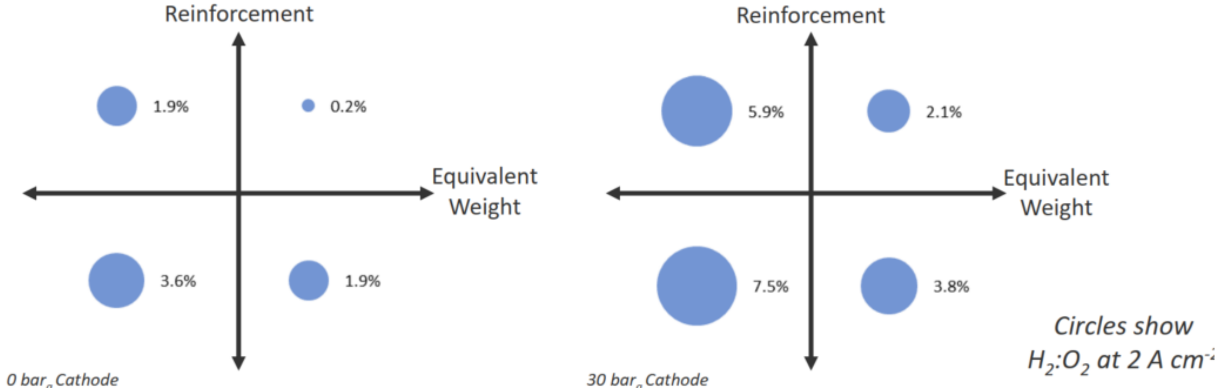

Figure 6. Parametric evaluation of 50 µm composite membranes containing two Nafion™ polymer equivalent weights and ePTFE reinforcements.

A lower polymer EW in the composite membrane resulted in a higher H_2 in O_2 content at both 0 and 30 bar, and for each ePTFE reinforcement tested. This observation is consistent with observed trends in neat Nafion™ films, where permeability has increased with decreasing EW. It is understood that increased water content resulting from lower EW (higher sulfonic acid content on a molar basis) facilitates gas crossover in the membrane. With regard to reinforcement, it can be seen that a higher reinforcement content reduces hydrogen crossover. The permeability of PTFE is around an order of magnitude lower than Nafion™, so it is intuitive that a higher weight/volume fraction of non-conductive, non-water-containing PTFE reinforcement would represent an enhanced barrier to gas crossover. However, the increased non-conductive content also reduces proton transport, so a trade-off between gas crossover, proton transport, and membrane strength is critical to design of an optimized membrane.

A similar evaluation was undertaken at LANL in an ex-situ cell (described in section 3.1) and is shown in Figure 7. The effects studied (See Table 3) are polymer equivalent weight and reinforcement mass. Interestingly, in this ex-situ cell configuration, the variation within the parameters studied was not sufficient to yield a meaningful/statistically significant difference in hydrogen permeability (unmitigated by GRC) in a 50 micrometer thick membrane. This contrasts with the above *operando* results where measurable differences were observed, and suggests a difference between the in-situ/ex-situ evaluation methods as discussed in the conclusion.

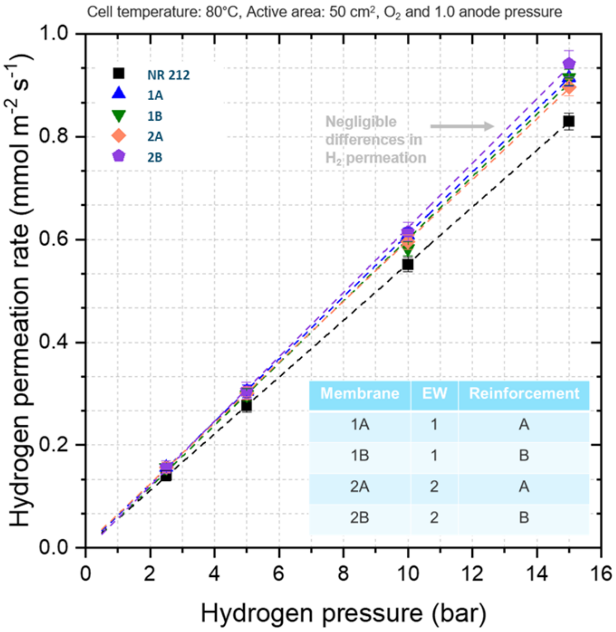

Membrane	EW	Reinforcement
1A	1	A
1B	1	B
2A	2	A
2B	2	B

Figure 7. Hydrogen permeation as a function of membrane composition for a series of unmitigated membranes in the LANL ex-situ cell

2.3 Membrane Pilot Manufacturing and Scale Up

An early version of the membrane concept shown in Figure 3 was successfully implemented on the Chemours pilot line for membrane fabrication, with SEM micrograph of the composite structure shown in Figure 8. The centered reinforcement, with sided GRC layer, is apparent in the micrograph. Optimization of GRC location and metal content was the subject of further work, but good promise was demonstrated that the fabrication scheme can extend into commercially relevant manufacturing.

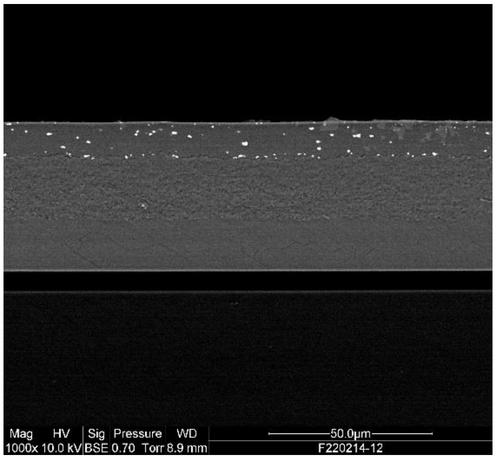

Figure 8. Cross section image of pilot scale membrane in SEM.

In Budget Period 2, Chemours focused on membrane fabrication with GRCs and reinforcements. Membranes were fabricated at both the lab scale and on Chemours' pilot coater. Table 4 below comprises a selection of membranes fabricated during the period that were shipped to collaborators for examination.

Table 4. GRC-containing membrane tested at NREL/LANL.

Membrane Tag	Thickness (μm)	Fabrication	GRC loading (μg/cm^2)	GRC Composition
C958-04-1 C958-05-1	50	Lab Scale	<75	A
C958-04-2	50	Pilot Scale	<75	B
C958-04-3	50	Pilot Scale	<75	B
C958-05-2	50	Lab Scale	<75	A
C958-05-3	50	Lab Scale	<75	A
C958-06-1	50	Lab Scale	<75	B
C958-06-2	50	Lab Scale	<75	B
C958-06-3	50	Lab Scale	<75	B

As membrane candidates were evaluated in the second year of the project, compositions were down-selected leveraging work from the above table and pilot membrane manufacturing runs at-scale were completed. These pilot scale membranes are evaluated throughout the document and are described in Table 5 below.

Table 5. Pilot Membrane Runs at Chemours Coater.

Membrane Tag	Thickness (μm)	Fabrication	GRC loading (μg/cm^2)	GRC Composition	Length (m)
22-1X Pilot Membrane 1	50	Pilot Scale	<75	A	10
30-1X Pilot Membrane 2	50	Pilot Scale	<75	B	10
38-2X Pilot Membrane 3	50	Pilot Scale	<75	C	20

3. Membrane Characterization in Ex-Situ Methods

3.1 Ex-Situ Gas Crossover Test Cell

The H_2 crossover measurements were conducted using a cell hardware with an active area of 5 or 50 cm^2 with single-channel serpentine flow channel configuration. Mass flow controllers are placed in-line prior to the cell inlets to precisely control the flowrate of 200 standard cm^3 (sccm) in both anode and cathode. Anode was supplied with 10 ml min^{-1} of water using a high performance liquid chromatography (HPLC) pump. The back pressure on the anode is varied to maintain a constant partial pressure of N_2 to be 1 atm, while the partial pressure of H_2 on the cathode was varied between 1 atm to 6 atm to create a pressure differential of 0 to 5 atm. The cell temperature was during the measurement was either 60 °C or 80 °C. The anode exhaust was connected to a condenser to remove water, where the dry output was then fed to a gas chromatograph (GC) to measure the concentration of hydrogen in the cathode exhaust gas as a percentage.

A schematic of the set-up is depicted in Figure 9 below. The cell hardware contains a membrane (without electrodes) placed between porous transport layers (from Bekaert) in a 5 or 50cm2 test fixture. The actual hardware at LANL is pictured in Figure 10.

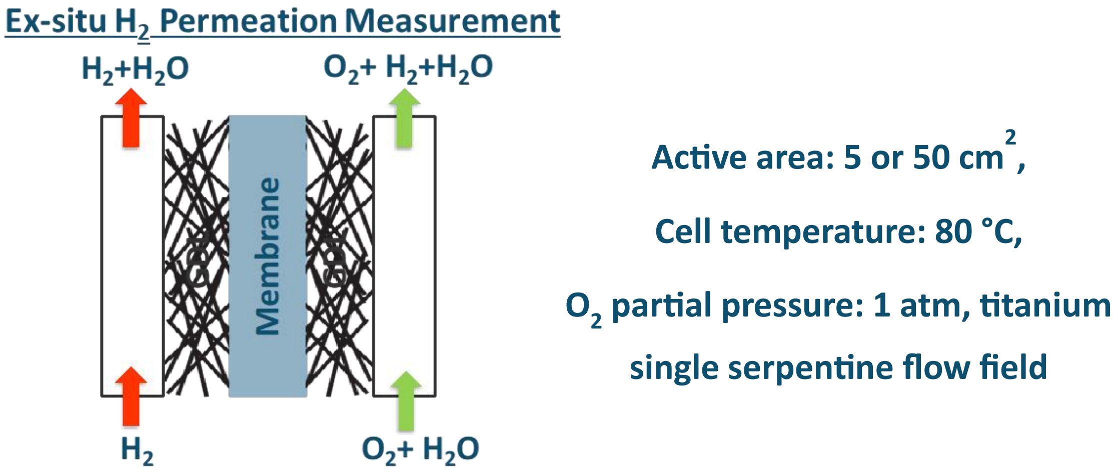

Figure 9. Ex-situ permeation cell set-up from LANL. Maximum H2 pressure is 6 atm. Oxygen is supersaturated.

Figure 10: Experimental setup for H_2 crossover measurement using gas chromatography for ex-situ method at LANL

Results for the 4 baseline membranes described in Section 2.2, along with a prototype lab-scale membrane 773-14-2 containing a GRC (from process C described above), were tested in this set-up with results shown in Figure 11 below and tabulated in Table 6. For membranes without GRC, the hydrogen crossover appears to be a strong function of thickness as expected. As a function of pressure, all are linear (again, expected). However, the GRC-containing membrane appears to be effective at reducing the amount of hydrogen contained in the oxygen stream up to ~3x between 1-6 atm H_2. While only a moderate reduction, this early promising result suggests that the GRC technique is able to reduce the “effective” hydrogen crossover in a PEMWE membrane and that this ex-situ capability can reasonably quantify changes.

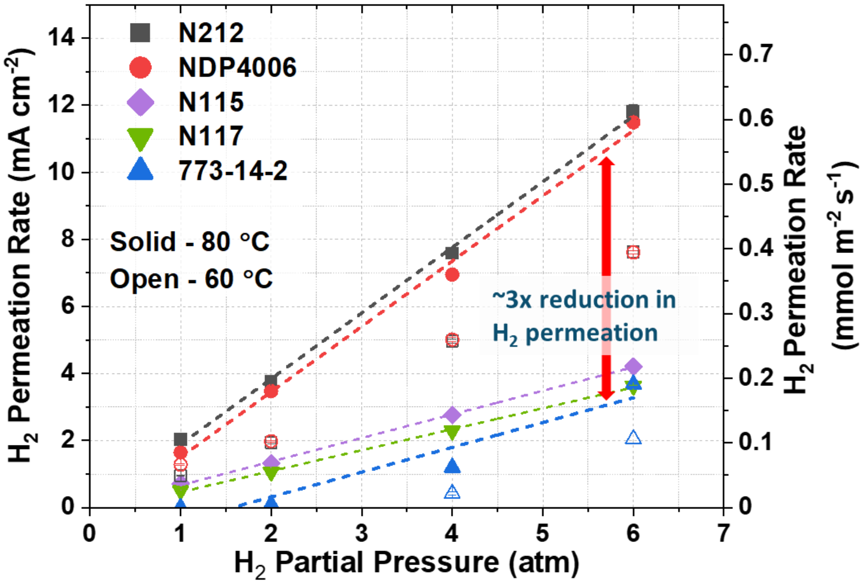

Figure 11. Effective gas crossover as a function of hydrogen partial pressure (see Figure 2 for cell and operating conditions).

Table 6. Baseline Effective H2 Crossover for Baseline Membranes and Early Prototype Membrane with GRC.

Membrane	Thickness (µm)	GRC Loading (mg/cm^2)	H_2 Permeation rate (mmol m^{-2} s^{-1} atm^{-1})
NR212	50	n/a	0.10
NDP 4006	50	n/a	0.10
N115	125	n/a	0.04
N117	175	n/a	0.03
773-14-2	~56	<<0.1	0.04

At LANL, the ex-situ hydrogen crossover cell was used to screen the crossover of 6 membranes from Table 4 in section 2.2: C958-05-(1-3), and C958-06-(1-3). The objective of the study was to understand the effect of GRC loading for two different GRC compositions. The results are depicted in Figure 12 below, with NDP 4006 (GRC-free, 50 micron reinforced pilot scale membrane) as a reference. As can be seen, the GRC-containing membranes reduce effective hydrogen crossover by between 5-10 times. Within the differential pressure window enabled by the cell, it is difficult to discern a difference in effective crossover as a function of GRC loading for the C958-05-(1-3) membranes. It should be noted that all membranes in the set C958-06-X developed pinholes between the 1-2 bar differential H_2 pressure steps and are thus not pictured below. These data partially satisfy **Milestone M3:** Manufacture membranes with at least 3 different additives for gas recombination and radical scavenging and evaluate their activity for H2 and O2 recombination/radical scavenging by monitoring H2 in O2 content and FER, respectively, at beginning of life (BoL) targeting 2% H2 in O2 for all current densities between 0.5 and 2 A/cm2 and an FER <0.25 µg/cm2-hr, a factor of 40x lower than NR211 in the DOE fuel cell combined chemical/mechanical AST.

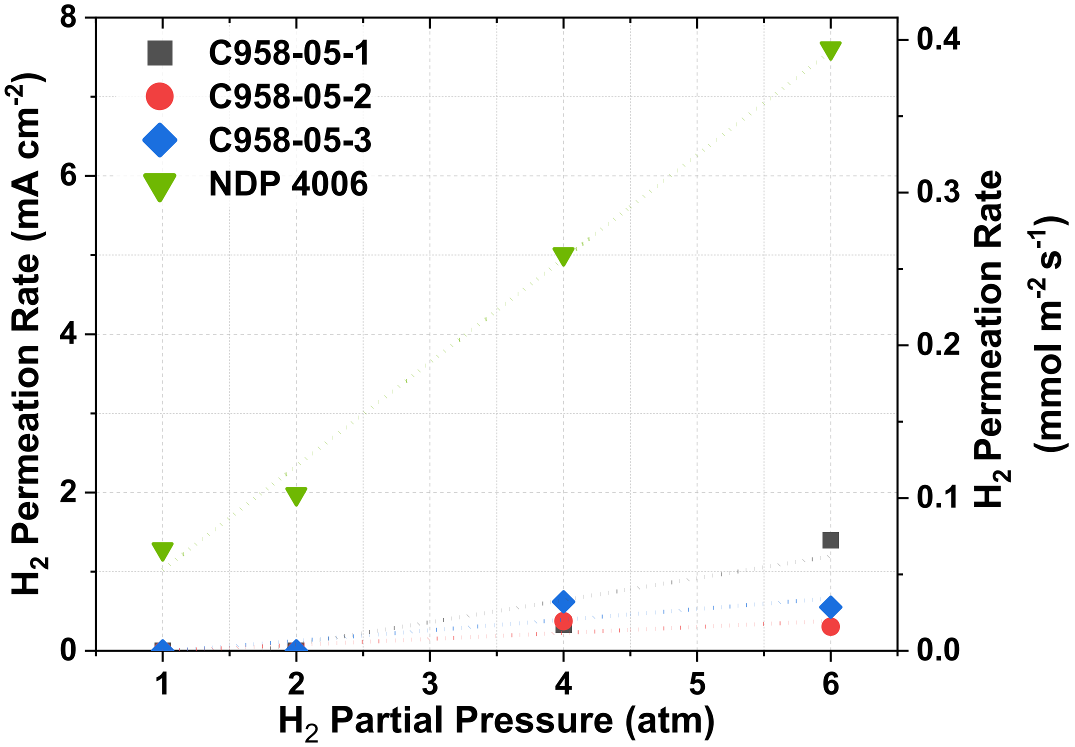

Figure 12. Ex-situ permeation cell results from LANL. Maximum H_2 pressure is 6 atm due to low cell pressure rating. Oxygen is supersaturated.

A limitation of the above cell is the pressure limitation of 6 bar at the cathode. This restriction was inherent to the cell design, as it was borrowed from fuel cell work and not rated at PEMWE relevant pressures. PEMWE environments often comprise a cathodic backpressure of 30 bar, which was the target cell cathode pressure for the project.

LANL adapted the ex-situ hydrogen crossover cell to enable testing from 1-30 bar hydrogen partial pressure by purchasing a new, high pressure cell from Greenlight. As received, membrane puncture was common in the cell hardware and significant effort was spent to address premature pinhole formation of thin membranes at intermediate pressures due to puncturing from PTL fibers. The surface of the PTLs were physically ground on a sander to smooth the surface to attempt to prevent pinhole formation, and sub-gasketing was utilized to avoid PTL from causing mechanical stress on the membrane. The first cell was ultimately replaced with a new design to enable interchangeable PTLs, but the mitigation techniques were maintained. While some tests below were reported at 30 bar, a high failure rate eventually required keeping the cell at 15 bar hydrogen pressure.

Results from the same baseline membranes studied to this point are presented in Figure 13. The expected linear relationships with hydrogen partial pressure are found. In Figure 14, the permeation rate (slope) from Figure 1 is plotted against inverse membrane thickness for membranes comprising only Nafion™ polymer. The linear relationship and low y-intercept (0 thickness) suggest that gas crossover in the high pressure cell is measured as expected from 0-30 bar when GRC mitigation is not present.

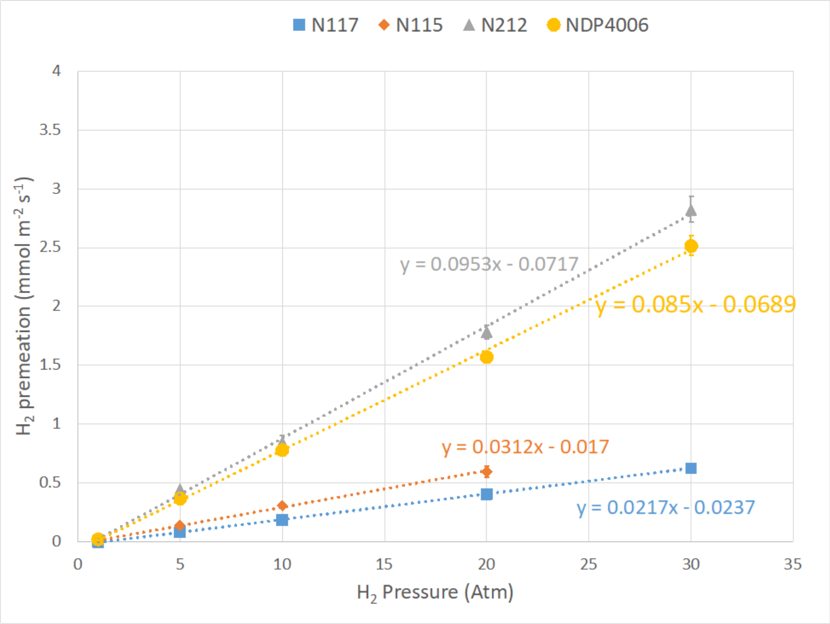

Figure 13. H2 permeation for N117, N115, NR212, and NDP 4006 as function of the H2 partial pressure. The anode pressure was maintained at 1 bar and the cell temperature at 80 °C.

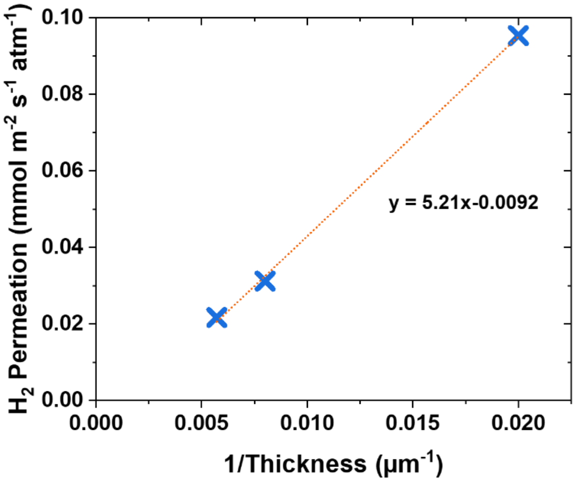

Figure 14. Unreinforced membrane permeation as a function of inverse thickness

LANL extended the high pressure cell capability to several pilot scale membranes, including membranes containing a GRC, with results presented in Figure 15. All membranes in the red oval are 50 µm in thickness with ePTFE reinforcement, made on Chemours' pilot line. Surprisingly, irrespective of GRC content, the observed hydrogen in oxygen concentrations are consistent for all membranes. Apparently, the GRC is inactive in the ex-situ screening cell as constructed, as GRC activity was confirmed several times in previous work at lower pressures.

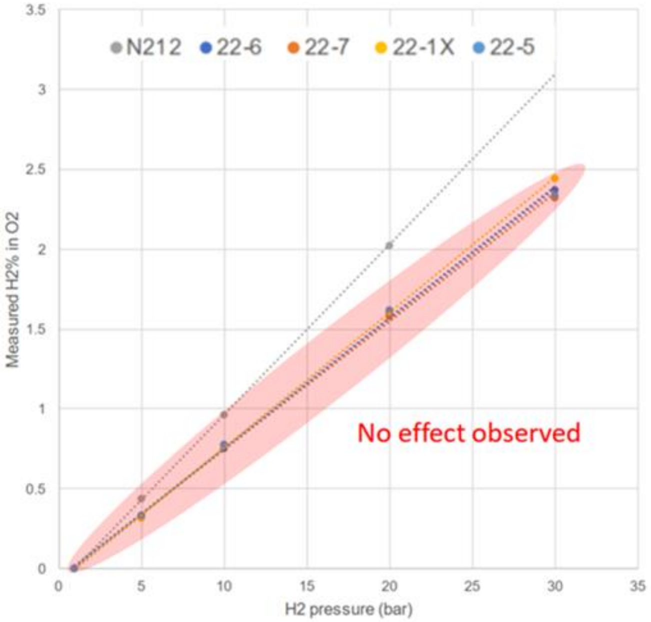

Figure 15. Crossover hydrogen as a function of H2 backpressure in an ex-situ screening cell at LANL.

Significant work was done to explore parameters within the ex-situ crossover cell to improve the "activation" of the GRC layer. Effects on permeation rate for NR212 and GRC-containing membrane samples were explored as a function of water flow rate and oxygen backpressure. A series of experiments were performed in both H_2/N_2 and H_2/O_2 environments to intentionally "deactivate" the GRC within the GRC-containing membrane, as oxygen is required for the recombination reaction to take place.

Figure 16 presents the difference between oxygen and nitrogen environments for the NR212 (no GRC) and 22-1X (GRC) membranes at a low and high flow rate of water. A small effect on hydrogen permeation is observed even in nitrogen for both membranes, where a higher water flow rate results in reduced crossover. This effect is possibly a result of enhanced local hydration of the membrane, which could increase membrane thickness through swelling and reduce gas crossover. The most obvious effect, however, comes from the GRC-containing membrane in oxygen (where a reduction in effective hydrogen permeation is expected). At low water flow rate, the difference between a nitrogen environment (inactive GRC) and oxygen environment (active GRC) is minimal. However, at the high flow rate, the magnitude of difference is substantially higher. The cause of this result is unclear.

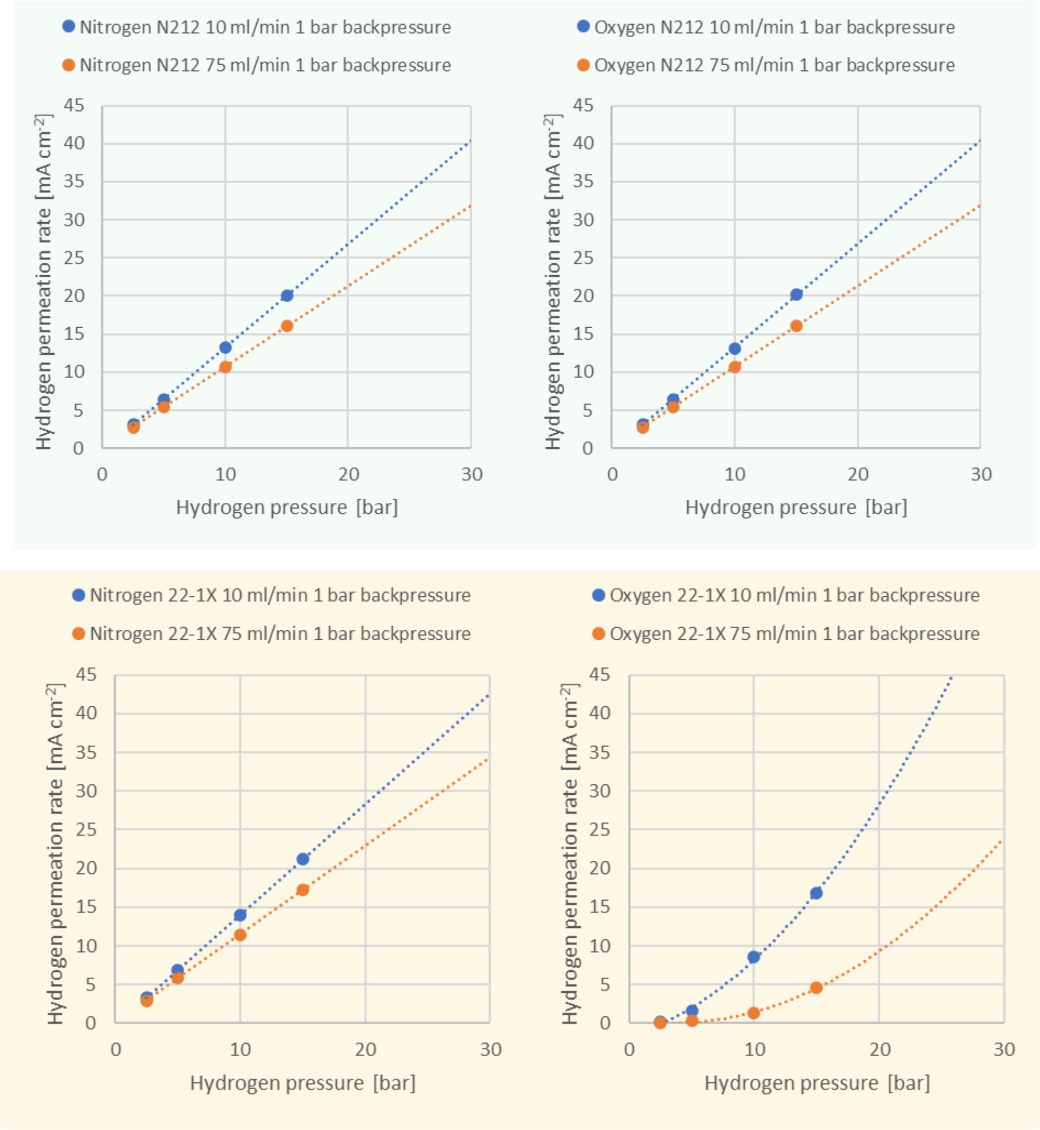

Figure 16. Permeation as a function of hydrogen backpressure for NR212 (top, no-GRC control) and 22-1X (bottom, GRC-containing sample) where ‘anode’ gas and water flow rate were varied.

In Figure 17, the effect of oxygen backpressure and water flow rate is summarized. The gap in crossover reduction between low and high water flow rate is presented for oxygen applied partial pressures of 1 and 4 bar. For membranes subjected to each pressure, reduced hydrogen crossover is noted, suggesting oxygen concentration is limiting for the overall recombination reaction in the ex-situ hardware.

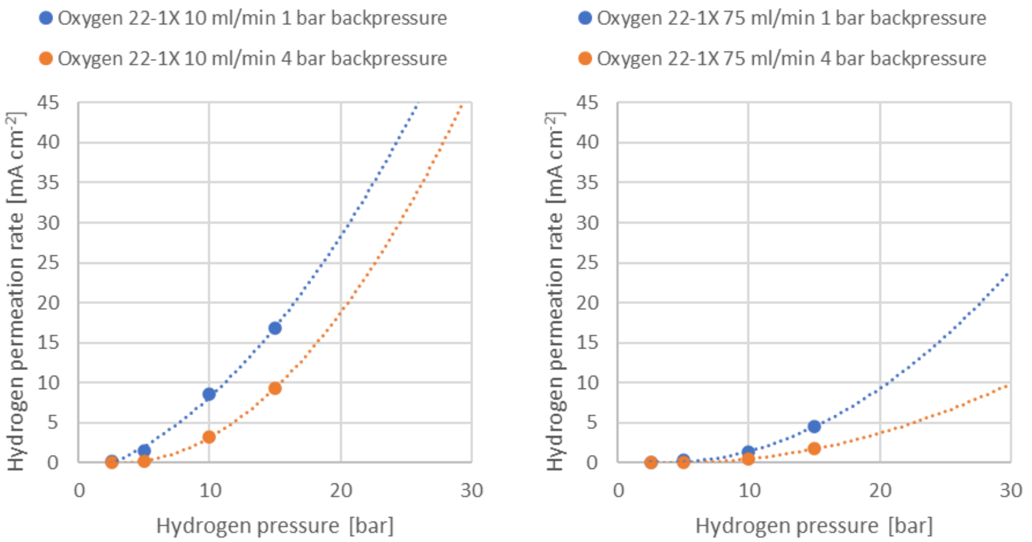

Figure 17. Effect of oxygen backpressure and water flow rate on GRC behavior in 22-1X membrane.

The difference between unmitigated hydrogen permeation (nitrogen atmosphere) and mitigated hydrogen permeation (oxygen atmosphere) at high water flow rate (75 mL/min) and high oxygen partial pressure (4 bar) is presented in Figure 18 for the GRC-containing membrane 22-1X. A factor of ten difference is measured in the rate of hydrogen permeation, which is a significant improvement over initial results in Figure 15 where no change was observed.

However, it should be noted that the magnitude of difference still does not match the operando data determined by NREL for application-relevant uses in Section 4 (where a ~50x difference in effective hydrogen permeation is found for this membrane). Further discussion on this topic is contained in suggestions for future work.

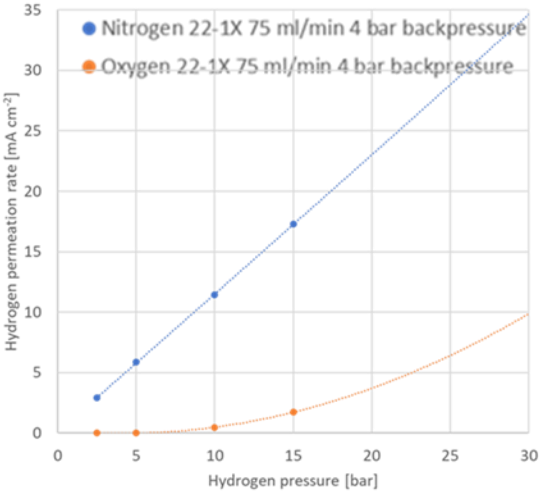

Figure 18. 10x reduction in hydrogen permeation between inactive and active GRC on 22-1X membrane.

Although the ex-situ capability was not determined to match the operando results, the cell was operated for a 1000 hour run on a single membrane to explore the variation of crossover over time. Pilot membrane 3 (38-2X), the best performer in terms of MEA polarization/crossover, was chosen for the test. Pressure was held at 15 bar on the cathode and 1 bar on the anode (each N2 gas). Water flow rate was 75 mL/min. Periodically, H2 and O2 were applied to the membrane and crossover was determined. The results in Figure 19 show that crossover was essentially consistent for 1000 hours, suggesting that simple compression without current density applied (in an operating MEA) is insufficient to effect the changes observed in an MEA environment.

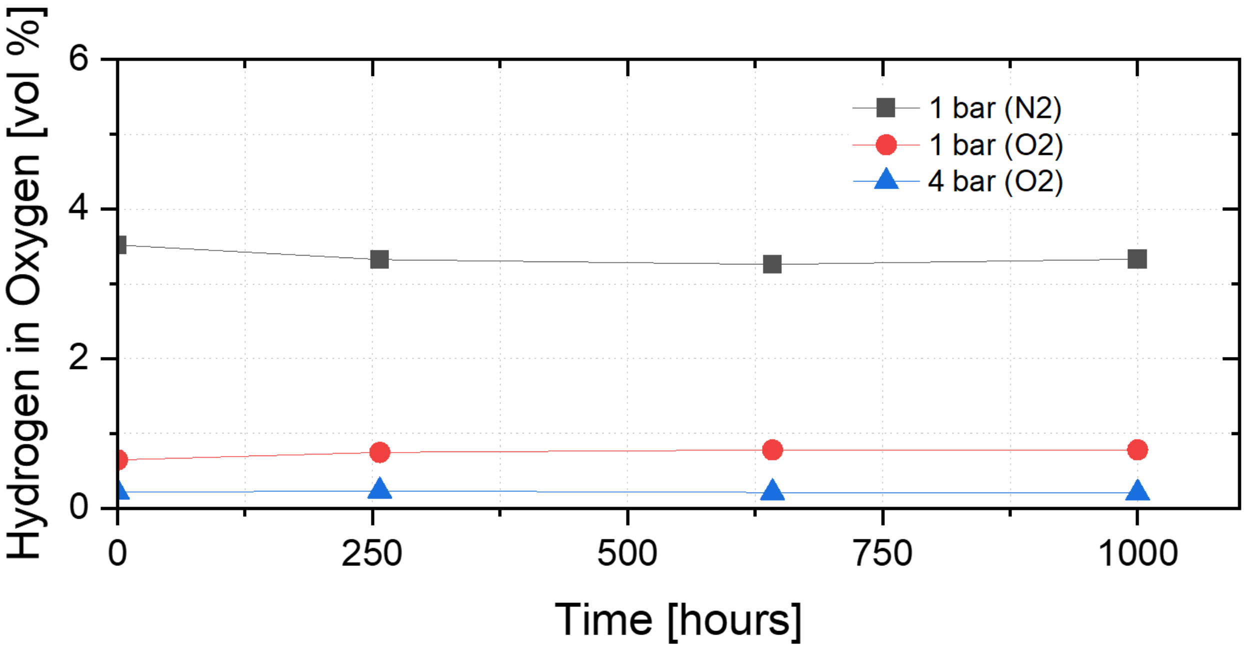

Figure 19. Ex-situ crossover test run for 1000 hours for 38-2X membrane.

3.2 Additive Mobility

In addition to the crossover cell, work was done at LANL to explore GRC and radical scavenger mobility within the membrane in the x-y plane. A spot testing X-ray fluorescence (XRF) tool was utilized to determine the GRC content in a small spot (100 x 100 µm) or a larger area map (5 cm^2). XRF testing was done for membranes used in ex-situ crossover experiments and was taken before and after the crossover test. An example XRF result is shown in Figure 20, where a consistent GRC loading is found across the area tested (100 x 100 µm). The membrane tested (773-10-6) is an example of a very early GRC membrane from process C described in section 2.1. The membrane thickness was 55 µm and it did not contain reinforcement.

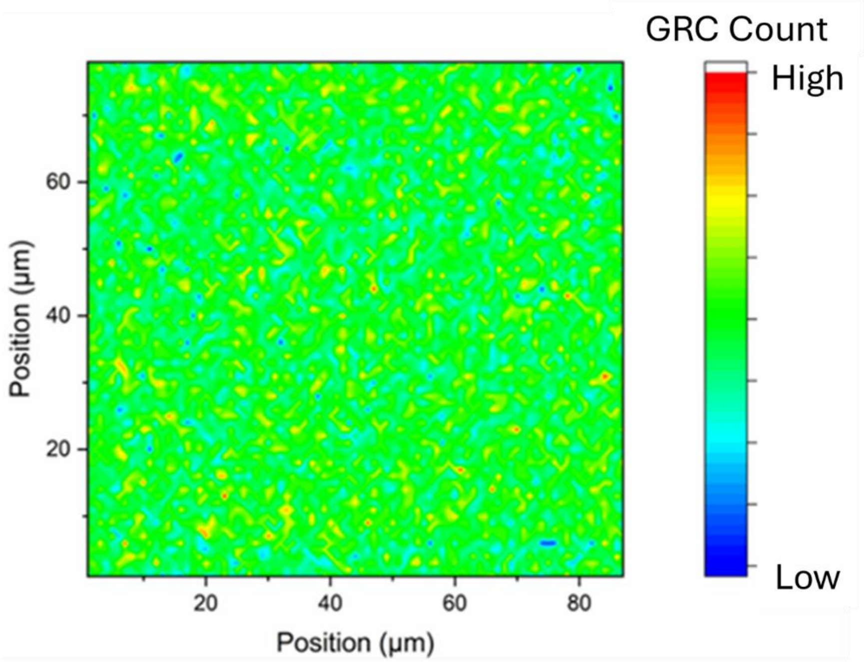

Figure 20. GRC distribution for 773-10-6 membrane.

Figures 21 and 22 show the testing profile and end-of-life GRC distribution for 773-10-6 subjected to H_2/O_2 (figure 21) and N_2/N_2 (Figure 22) environments in the ex-situ cell. These tests were intended to simulate the recombination reaction and associated local water production that occurs in a PEMWE cell, compared to a control with an inactive GRC (N_2/N_2). The GRC appears to move from the bulk of the membrane toward the perimeter of the active area after exposure to H_2/O_2 where local water generation via recombination hydrates the local environment around the GRC. However, this effect is not observed in N_2/N_2 control testing where the recombination reaction is inactive.

This unexpected result suggests that a risk of GRC-containing membranes is the movement of the GRC during operation in an MEA (i.e., when exposed to current density or temperature cycles). As the static location of GRC within the membrane over its lifetime is critical to crossover mitigation, improvement of this observed mobility is required. One potential explanation of the observed effect is the small domain size of the GRC in this membrane, which could facilitate movement within the Nafion™ polymer water channels.

- 773-10-6 membrane
- Assembled in 5 cm^2 cell
  - membrane with no catalyst
  - PTL
- Cell at 65 ˚C
- Cathode: Dry H_2 @30 psi backpressure
- Anode: Highly humidified O_2 (90 ˚C) + H_2O at 3 ml min^{-1} @ 0 psi backpressure

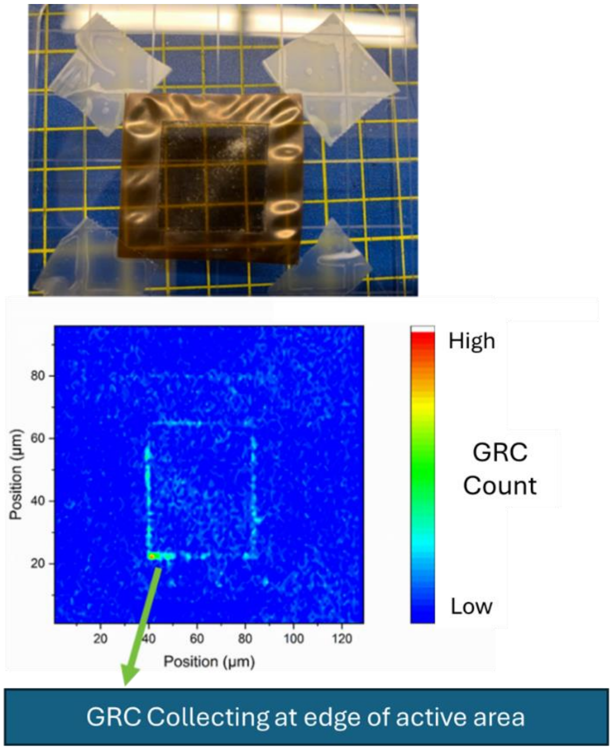

GRC Collecting at edge of active area

Figure 21. GRC mobility in a supersaturated H_2/O_2 environment

- 773-10-6 membrane
- Assembled in 5 cm2 cell
  - membrane with no catalyst
  - PTL
- Cell at 65 ˚C
- Cathode: Dry N2 @30 psi backpressure
- Highly humidified N2 (90 ˚C) + H2O at 3 ml min^{-1} @ 0 psi backpressure

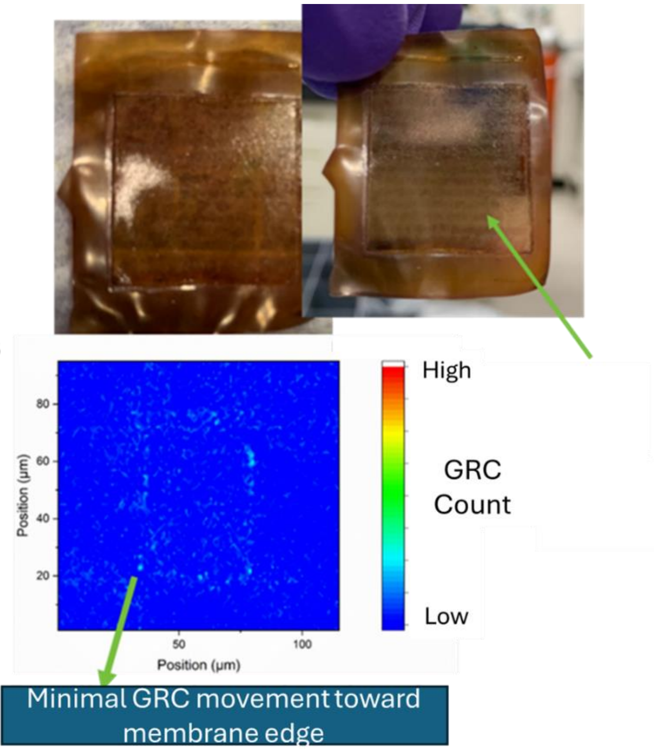

Minimal GRC movement toward membrane edge

Figure 22. GRC mobility in a supersaturated N_2/N_2 environment

For the revised series of membranes described in Table 4, XRF was utilized to evaluate depletion of the GRC resulting from movement within/out of the membrane. Several spots in the active (blue) and inactive (black) areas of a given membrane were evaluated for GRC loading before and after a recombination experiment in the ex-situ cell. Figure 23 displays the testing locations, and Tables 7 & 8 give the GRC loading results for each spot.

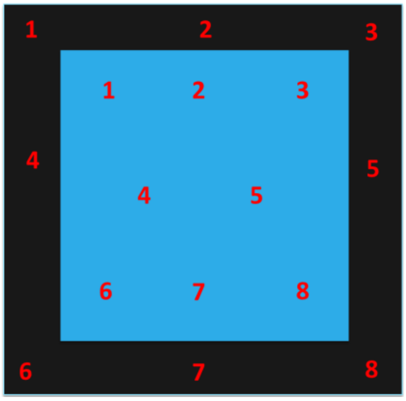

Figure 23. XRF Spot Testing Map for Post-Crossover-Test Membranes at LANL

Table 7. C958-05-1 Spot XRF Results. GRC average loading normalized to 100%.

Spot #	Inside Active Area (μg cm^{-2})	Outside Active area (μg cm^{-2})
1	96.4%	105.4%
2	98.1%	107.3%
3	101.9%	87.6%
4	106.7%	88.6%
5	92.2%	108.5%
6	106.2%	96.6%
7	103.1%	111.5%
8	95.5%	94.5%
Average	100.0%	100.6%

Table 8. C958-05-2 Spot XRF Results. GRC average loading normalized to 100%.

Spot #	Inside Active Area (µg cm^{-2})	Outside Active area (µg cm^{-2})
1	104.2%	115.1%
2	95.7%	101.6%
3	105.4%	113.2%
4	100.7%	113.1%
5	93.9%	88.5%
6	96.2%	100.8%
7	96.3%	88.6%
8	107.7%	79.1%
Average	100.0%	100.2%

As can be seen, the spot test XRF results for two separate membranes show no meaningful difference in the average GRC loadings inside and outside the active area for recombination at the conclusion of the crossover test. Also, there appears to be no meaningful difference with respect to position within the active or inactive areas. These findings suggest a lack of GRC movement in the membrane, counter to the initial result that demonstrated a severe accumulation/depletion within the active area.

Some concepts for PEMWE membranes contain a radical scavenger, which is intended to mitigate oxidative attack similar to those found in fuel cell membranes. In figure 24, a test is performed (adapted from Reference 6) where the radical scavenger is encouraged to move in a high voltage environment. The membrane is immersed in 85C liquid water, and a voltage gradient is applied to a membrane containing various compositions of radical scavengers in a BekkTech cell. The voltage applied is effective to enable movement of radical scavengers in fuel cell literature (e.g., cerium salts). One tested scavenger is completely immobile in the test procedure, which is promising for reduced mobility in PEMWE application. These data are in partial fulfillment of **Milestone M3**: *Manufacture membranes with at least 3 different additives for gas recombination and radical scavenging and evaluate their activity for H2 and O2 recombination/radical scavenging by monitoring H2 in O2 content and Fluoride Emission Rate (FER), respectively, at beginning of life (BoL) targeting 2% H2 in O2 for all current densities between 0.5 and 2 A/cm2 and an FER <0.25 µg/cm2-hr, a factor of 40x lower than NR211 in the DOE fuel cell combined chemical/mechanical AST.*

It should be noted that test stations for PEMWE FER testing were not available during the project due to significant industry bandwidth limitations and this was not pursued in the project in alignment with DOE Project Management. Furthermore, iron tolerance testing was an aspirational capability intended to be developed, but which was impacted by LANL staffing departures in the early stages of the project. These limitations also apply to **Milestone M5**: *Begin AST testing of roll to roll fabricated reinforced membranes; quantify membrane FER to evaluate effect of different radical scavenger composition/loading with target FER <0.1 µg/cm2-hr* and **Milestone M11:** *Finish AST testing on down-selected material set giving > 10 mg/L Fe(III) tolerance and maintaining > 50% concentration of the radical scavenger in the membrane. Report on retention/mobility of GRC and radical scavengers in water wet PEMWE condition. Report FER from PEMWE-specific AST.*

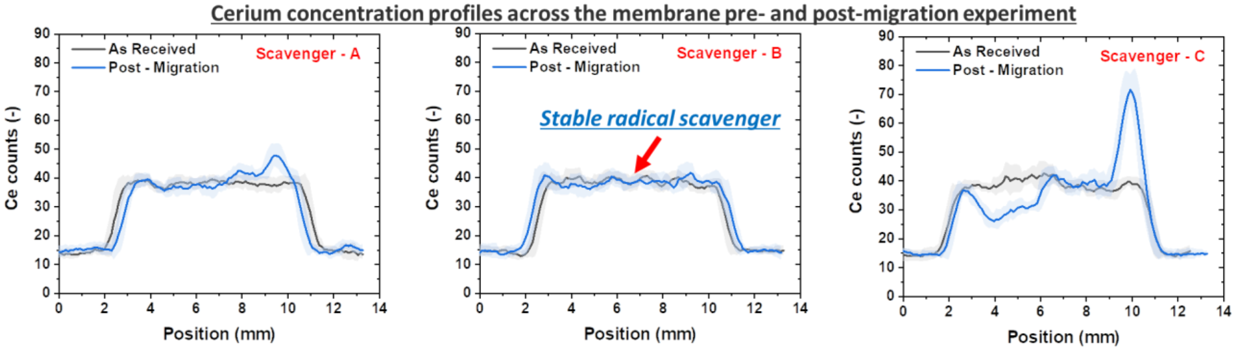

Figure 24. Radical Scavenger mobility in 85°C water.

4. Membrane Evaluation in an Electrolyzer

4.1 Crossover Measurement in an Operating Membrane Electrode Assembly (MEA)

HydroGEN node partner National Renewable Energy Lab (NREL) was tasked to leverage their world-class PEMWE MEA testing lab in this project, and to develop new capabilities to enable the polarization and crossover determination of operando MEAs at high cathodic pressure.

Within the first year of the project, NREL completed the design and customization process of a test stand for collecting quasi-real time GC analysis of the effluent streams of a PEMWE MEA. Note that a GC instrument is extremely intolerant to H_2O.To enable this analysis, additional components were added to an existing Greenlight test station. A picture of the GL50 test station is shown in Figure a. No major modifications were made to the test stand; however, several components were added to the exhaust gas lines in order to remove all liquid and the majority of the vapor phase H2O from the anode exhaust stream: (i) The anode exhaust line was fed through a water dropout device to remove liquid water from the water/gas stream. (ii) Subsequently, the line was passed through a thermoelectric (Peltier effect) cooling device to lower the temperature of the gas to the lowest possible dew point. (iii) After passing through the Peltier cooler, the exhaust gas is passed through a second water dropout device to remove any remaining liquid water.

After these steps, the gas stream must be reheated for testing in the GC. Figure b shows the heated lines and PID temperature controllers for this process. Lastly, the gas is passed through pressure transducers to regulate its pressure before entering the GC. Figure c shows the backpressure regulators, heated tubing, thermocouple ports, and GC inlet contained in this final stage. Figure 26 shows a comprehensive schematic drawing of the added system components for effluent gas testing.

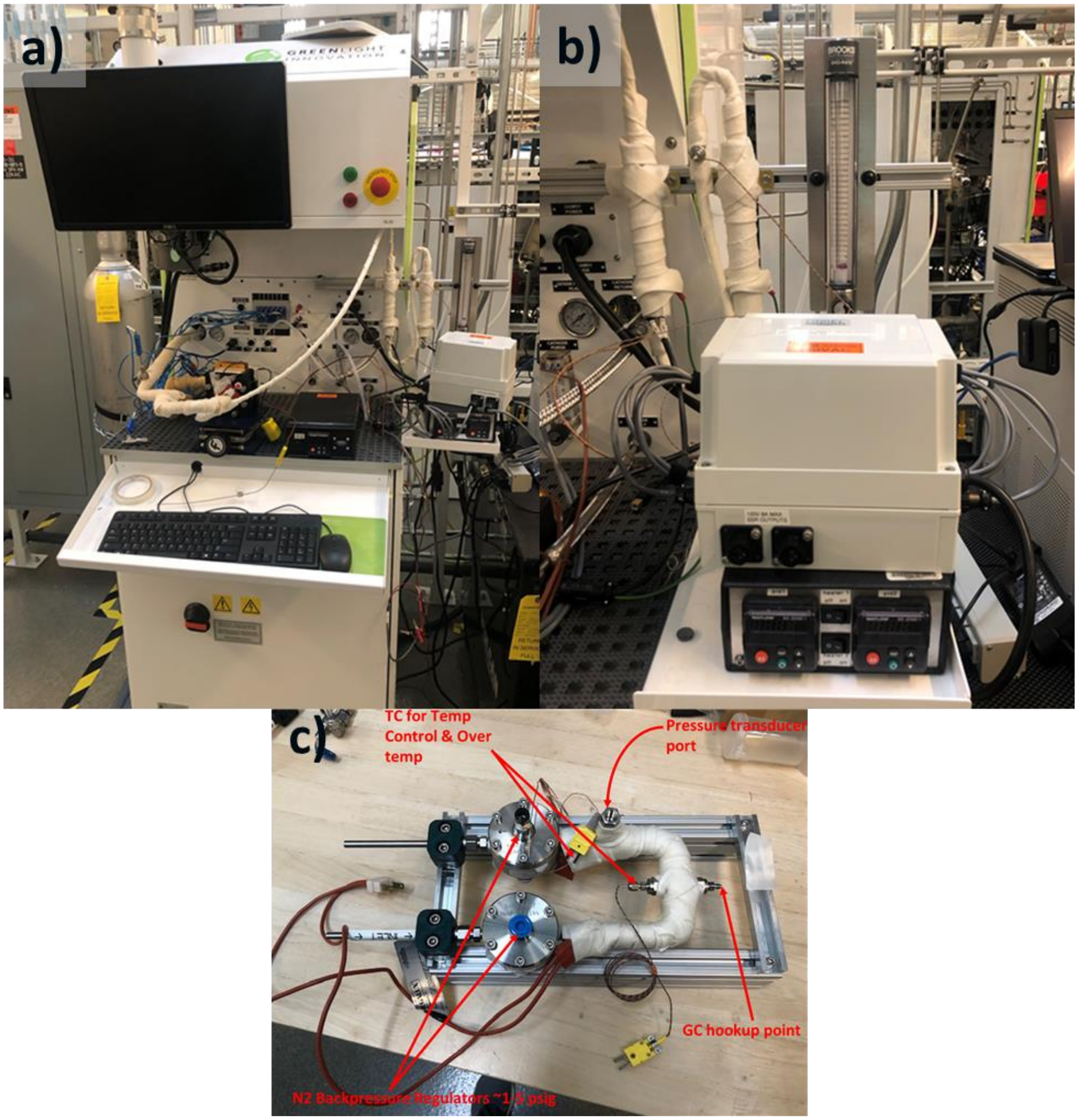

Figure 25. Pictures of test stand components, including a) Greenlight GL50 test station, b) heated transfer tubes and temperature PID controllers for GC inlet, and c) effluent stream pretreatment components leading up to the GC.

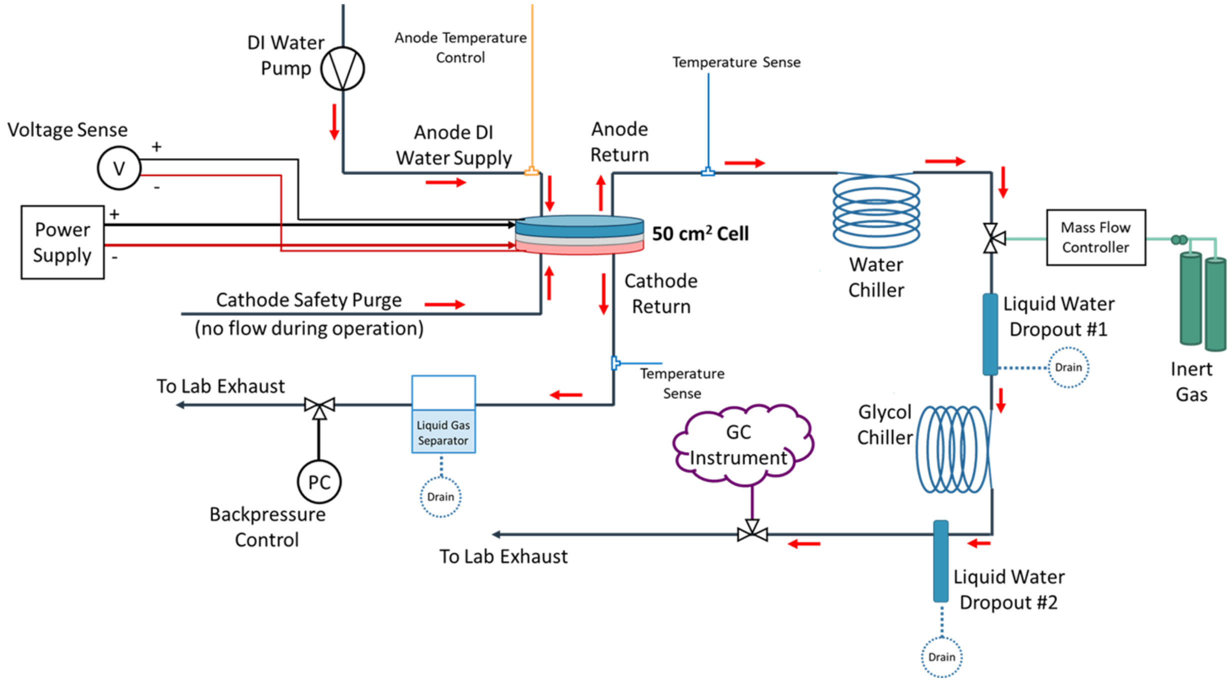

Figure 26. Scheme for PEMWE cell performance and hydrogen crossover determination by gas chromatograph at NREL.

Initially, NREL intended to use mass spectrometry (MS) to analyze the effluent gas stream, and an OmniStar™ ThermoStar™ GSD320 Gas Analysis System was implemented. However, during preliminary verification studies using a calibration sample, it was found that the MS system took a prohibitively long time to equilibrate and analyze the sample. After almost 3 hours, the signal had not reached steady state, rendering MS unsuitable for the proposed experiments. GC was selected as an alternative to MS. The GC measurements in Figure 27 were obtained after just a few minutes, which enables full scans of a current density range within a reasonable amount of time.

In order to measure the gas crossover of thin, experimental membranes, an inert gas carrier was implemented to dilute the (hydrogen-containing) oxygen stream after it exits the anode. This carrier gas allows quantification of gas streams that would otherwise contain too-high hydrogen contents to be allowed (for safety reasons). This is extremely important for thin membrane research, as initial prototypes of GRC-containing membranes are not required/expected to be 100% successful in reaching <2% hydrogen in oxygen concentrations. The quantification of MEA-based hydrogen crossover is critical to understanding its behavior for load-following applications. This concept is further explained in Figures 27 and 28 below.

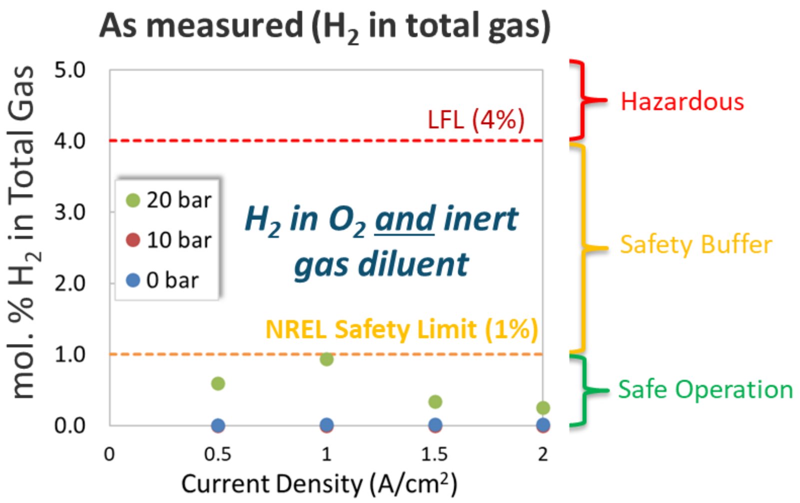

Figure 27. As-measured gas content in GC (containing inert gas diluent)

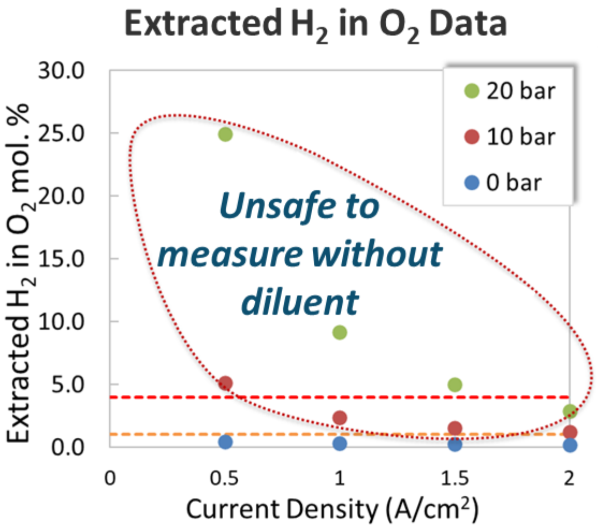

Figure 28. Adjusted Hydrogen in Oxygen content of anode stream once inert diluent content is compensated.

As the project progressed, NREL modified the original gas crossover quantification setup to be more physically streamlined. Figure 29 shows the more compact, portable configuration. A parts list was transferred to Chemours such that Chemours could re-construct the crossover cart for in-house testing after the duration of the project.

Figure 29. Revised crossover cart at NREL

4.2: MEA & Cell Hardware and Polarization Procedure

The materials set used in membrane electrode assemblies (MEAs) within this project is presented in Table 9. This table and section below serves to complete **Milestone M1**: *define initial electrolysis membrane MEA material sets and ASTs which are capable of providing performance of at least 2 A/cm2 at 1.9 V*. It was originally envisioned that ASTs would be leveraged in this project to probe membrane durability, but as discussed in later sections, equipment bandwidth was a consistent challenge that limited long-term testing availability. In alignment with DOE Program Management, the long-term testing that was performed instead focused on galvanostatic holds for hundreds of hours (please see section 4.3 below).

Several membranes are included to determine the impact of thickness on performance, which will inform the impact of a reinforcement on membrane transport properties. Also, gas crossover for unmodified membranes as a function of thickness clarified the effectiveness of a gas recombination catalyst. Catalysts are standard for PEMWE cells. Loading is aligned with H2NEW FuGeMEA[9] content and is a compromise between a low loading (to approximate state of the art in research labs) and high loading (to avoid catalyst limitations/degradation in evaluating membrane within the project). GDL/PTL materials are commercial and readily available.

Gas recombination catalysts (GRCs) and radical scavengers are not included in this baseline materials set as they were changed/optimized based on feedback over the scope of the project.

Table 9. Materials Sets for Membrane Electrode Assemblies to be Evaluated In Project

Component	Condition	Material/Amount
Membranes		N117 N115 NR212 (also labeled as N212) Additive free Reinforced Membrane (NDP 4006)
Electrode Catalyst	Anode	Iridium Oxide
	Cathode	Platinum on High Surface Area Carbon
Electrode Loading	Anode	0.4 mg/cm^2
	Cathode	0.1 mg/cm^2
Gas Diffusion Layer	Cathode	0% PTFE Carbon Paper (Toray)
Porous Transport Layer	Anode	Pt-Sputtered Titanium Felt (Bekaert) 2GDL5-0,125 or 2GDL6-0,25
Gaskets	Ambient Pressure	Polytetrafluoroethylene (PTFE)
	Differential Pressure	PTFE

NREL collected initial data on MEAs utilizing the high pressure Giner cell with a round MEA configuration. As H2NEW efforts increased in the later duration of the project, a square configuration hardware (modified from a Fuel Cell Technologies fuel cell build) was utilized. In each case, the active area was 50 cm^2. The circular design of the Giner cell required custom cutting dies and computer-controlled gasket cutting to create the required gasket sets MEA geometry for assembly and operation. All cells were tested on a Greenlight Innovation E30 test station (see Figure 25), which controls and automates the temperature, flow rate, current/voltage, and backpressure.

Figure 30 shows the time resolved data of the cell conditioning procedure (Figure 30a) and of polarization curves (Figure 30b) conducted with the cell builds. The break-in procedure consists of 30-minute galvanostatic holds at 0.2 A/cm^2 and 1.0 A/cm^2 followed by a potentiostatic hold at 1.7 V for 8-16 hours. Following the break-in, potentiostatic polarization curves are collected by holding each voltage for 5 minutes and taking the steady state current and voltage values. Initial experiments consist of voltage-controlled polarization curves to verify proper performance and cell integrity. Subsequent performance tests, utilizing test station automation, employed current-controlled operating modes. For the envisioned experimental matrix, current-controlled data is essential because the hydrogen crossover is governed by cell current. Current-controlled data facilitate comparisons across different cell designs and operating conditions. Initial current density ranges were 0.05 to 3 A/cm^2, but this was extended to 4 A/cm^2 to extend the testing range.

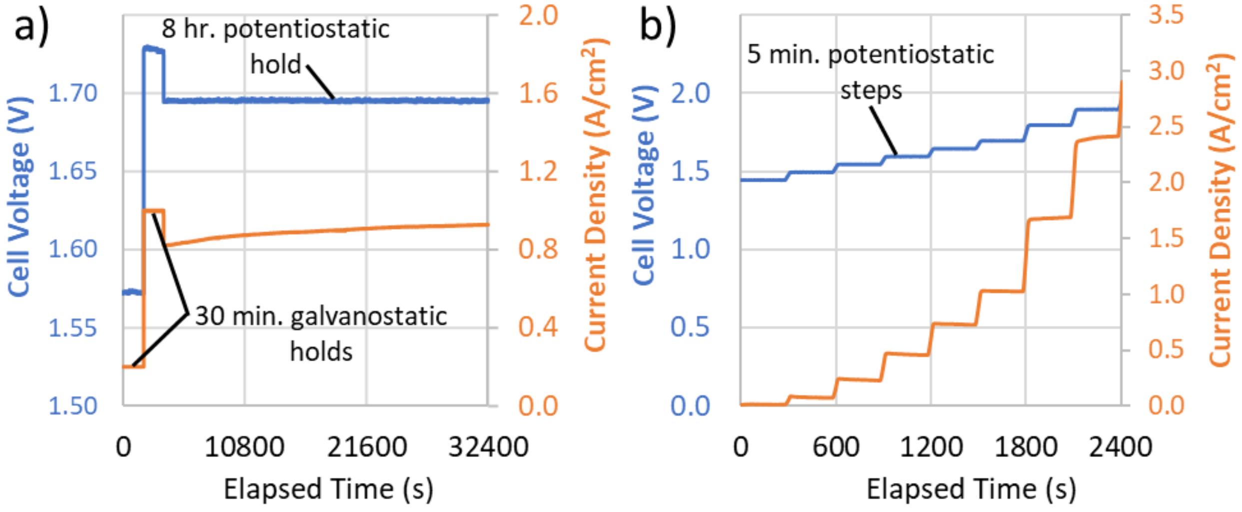

Figure 30. Time-varying plots showing the methodologies for the (a) MEA break-in procedure and (b) voltage-controlled polarization curves.

After the break-in procedure, polarization curves were collected at different operating conditions (temperature, pressure) to observe their effect on performance and verify that the test station was automated correctly. Figure 34 shows example results for an N115 membrane utilizing the materials set in Table 9. Polarization curves were obtained at 60°C and 80°C at cathode backpressures of ambient, 10 bar, 20 bar, and 30 bar. All tests used an anode water flow rate of 300 ml/min. In general, increasing the backpressure of cathodic hydrogen leads to lower current densities at the applied voltages (or less voltage at a given current density). This is due to a simple Nernstian effect, i.e., increasing the activity (partial pressure) of H_2 increases the anodic current of the HER, thereby increasing the overpotential.

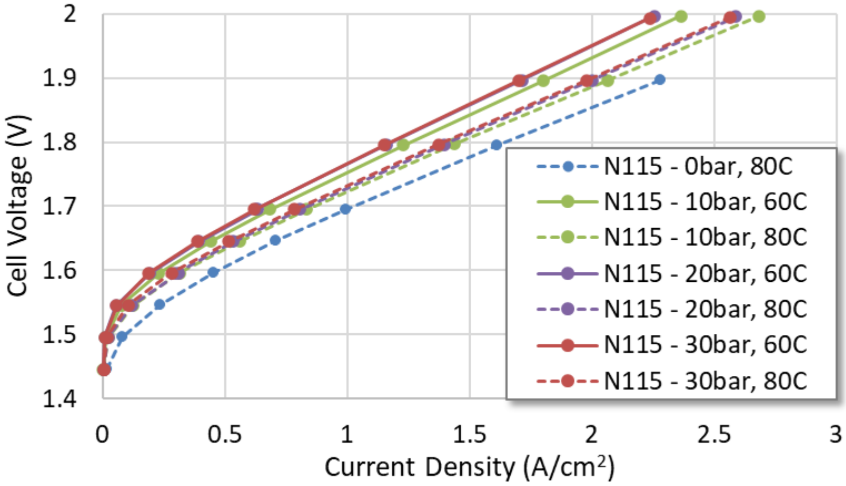

Figure 31. Polarization curves for an in-house N-115 MEA obtained at selected temperatures and differential pressures.

Even if all crossover hydrogen is recombined with oxygen in the membrane, it is not captured in the product stream and represents a loss to the overall faradaic (hydrogen) efficiency of the PEMWE stack. Reducing membrane thickness therefore introduces a tradeoff between improved performance (reduced ohmic losses, improved voltage efficiency) and decreased faradaic (hydrogen) efficiency (H2 losses to crossover, recombination). Equation 1 presents the calculation used to determine faradaic (hydrogen) efficiency, and equation 2 quantifies the energy consumption to make a kilogram of hydrogen. F is Faraday's constant, i is the current density (A/cm^2), A is cell area (cm), j is the crossover current for hydrogen (A/cm^2), V is voltage (V), and M is the molar mass of hydrogen.

Equation 1

$$\eta_{FE} = \frac{\dot{n}_{\mathrm{H}_2,usable}}{\dot{n}_{\mathrm{H}_2,actual}} = \frac{\frac{iA}{2F} - J_{H_2,xover}A}{\frac{iA}{2F}}$$

$$\boldsymbol{FE = 1 - \frac{2FJ_{H_2,xover}}{i}}$$

Equation 2

$$e_{\mathrm{H}_2}\left[\frac{J}{kg}\right] = \frac{P}{\dot{m}} = \frac{2FV}{(FE)M_{\mathrm{H}_2}}$$

4.3 Operando MEA Results with Prototype Membranes

Example polarization curves for the membranes in Table 2 are found in Figure 35 below. For the three commercial membranes, the trend of voltage with current density decreases in the order N117 > N115 > NR212. This tracks well with expectation, given that this is the order for decreasing proton transport resistance. N115 MEA shows an apparently slower break-in, as there is some "extra" activation-region energy loss in the first polarization regime that appears to be mediated by the 2nd and 3rd pol curves below.

Interestingly, NDP 4006, the experimental reinforced prototype membrane, demonstrates very good polarization results that meet or even exceed NR212. This is somewhat surprising given that NDP 4006 includes a non-charged reinforcement, though it does incorporate lower equivalent weight (EW) ionomer (<1000 EW) versus the 1000 EW Nafion™ used in the other 3 commercial membranes.

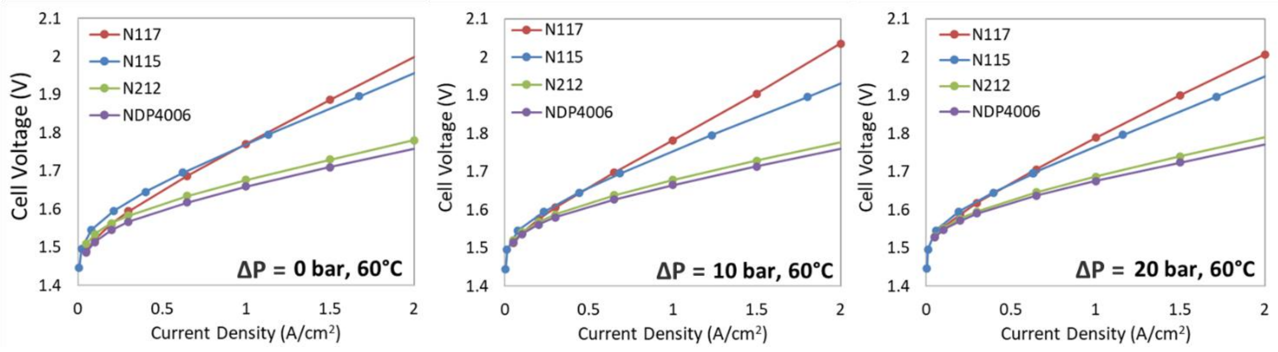

Figure 32. PEMWE polarization curves for 4 baseline membranes as a function of hydrogen backpressure.

The optimized membrane output (EW 1, reinforcement B) of the parametric analysis of EW and reinforcement described in Figure 5 was tested in an MEA using the FuGeMEA electrode platform described in Table 9. This membrane was taken to be the final project membrane performance, with results in Figure 33. The polarization curve matches well with the resistance results in Figure 5, as the new membrane exhibits a ~50 mV improvement at 3 A/cm2 that corresponds well to a 16 mOhm-cm^2 lower resistance from Figure 5. The polarization curve improvement appears to be ohmic driven (from HFR free voltage). These results describe the completion of **Milestone M9**: *Complete evaluation of low EW ionomers in reinforced membrane to determine impact of chemistry on operation temperature, performance, and durability of electrolyzer membrane leading to down-select decision on pursuing low EW ionomers.* The efficiency calculated by lower heating value (LHV) for a cell with the improved membrane is 72% at 3 A/cm^2, which is a significant improvement over the 60% value for N117 baseline membranes.

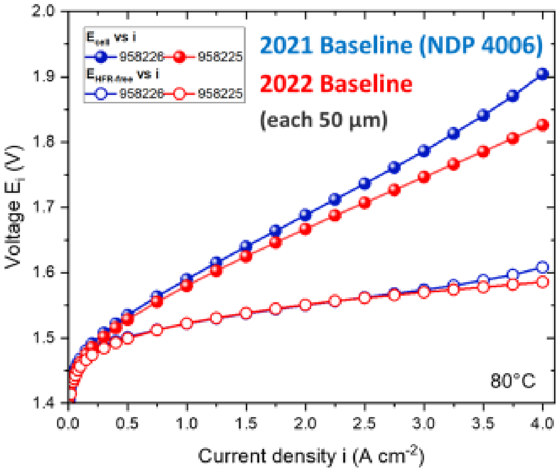

Figure 33. MEA and polarization curve testing parameters of two pilot scale membranes.

The consistency of this platform is depicted in Figure 34. For all prototype pilot line membranes, area specific resistance (ASR) is plotted as a function of sequential campaign number in Figure 34 below. While the exact value is obscured, the plateau of the ASR is <50 mOhm-cm^2. As can be seen, the performance of the membrane has settled in a consistent regime, representing a final composition in terms of reinforcement and ionomer EW. When evaluated in the FuGeMEA platform at NREL at 80°C and 0 bar H_2 back pressure, the performance of the membrane exceeds the 2026 DOE targets of 1.8 V @ 3 A/cm^2 (see inset).

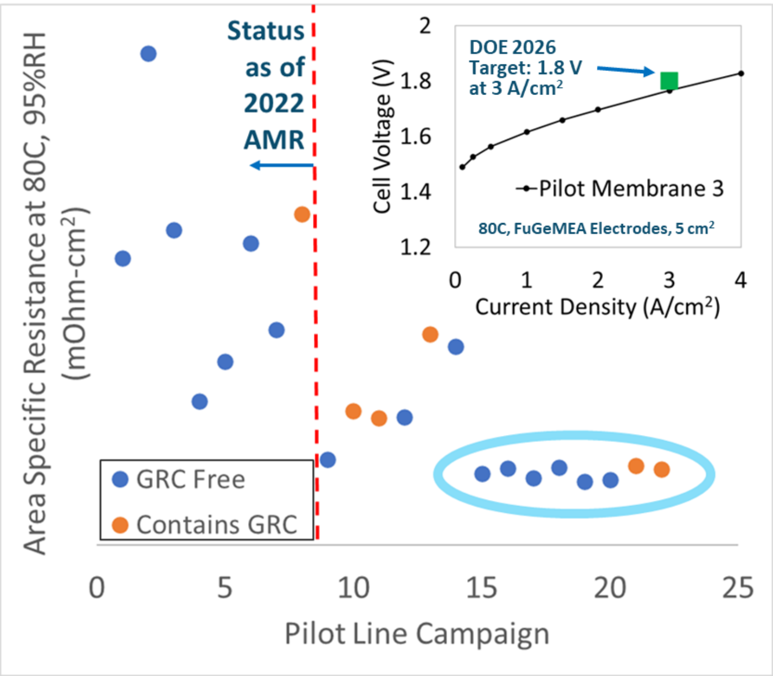

Figure 34. ASR of pilot line membranes as a function of campaign

Hydrogen crossover in operando MEAs is presented below in Figure 35 for the four baseline membranes without GRC. This serves as the completion of **Milestone M2**: *Establish test for gas crossover (H2 in O2 content) for electrolyzer MEAs, and acquire baseline crossover/performance for N115, N117, NR212-containing MEAs.* Operation temperatures were 60 and 80°C, and backpressure ranged from 0-20 bar. At 0 bar differential pressure (left), the hydrogen crossover for all membranes was well below the 4% H_2 in O_2 threshold for lower flammability limit. However, as hydrogen differential pressure increases (up to 20 bar), the amount of crossover gas detected by the GC dramatically increases. Especially for the thinner membranes, H_2 in O_2 content well above 4% is observed at lower current densities. The GRC concept is obviously required to mitigate this crossover in a high differential pressure, low proton resistance (thin) MEA that is expected to run for any time at low current density. It should be noted that these hydrogen/oxygen concentrations are safely measured within a nitrogen carrier gas as described in Figures 27 and 28.

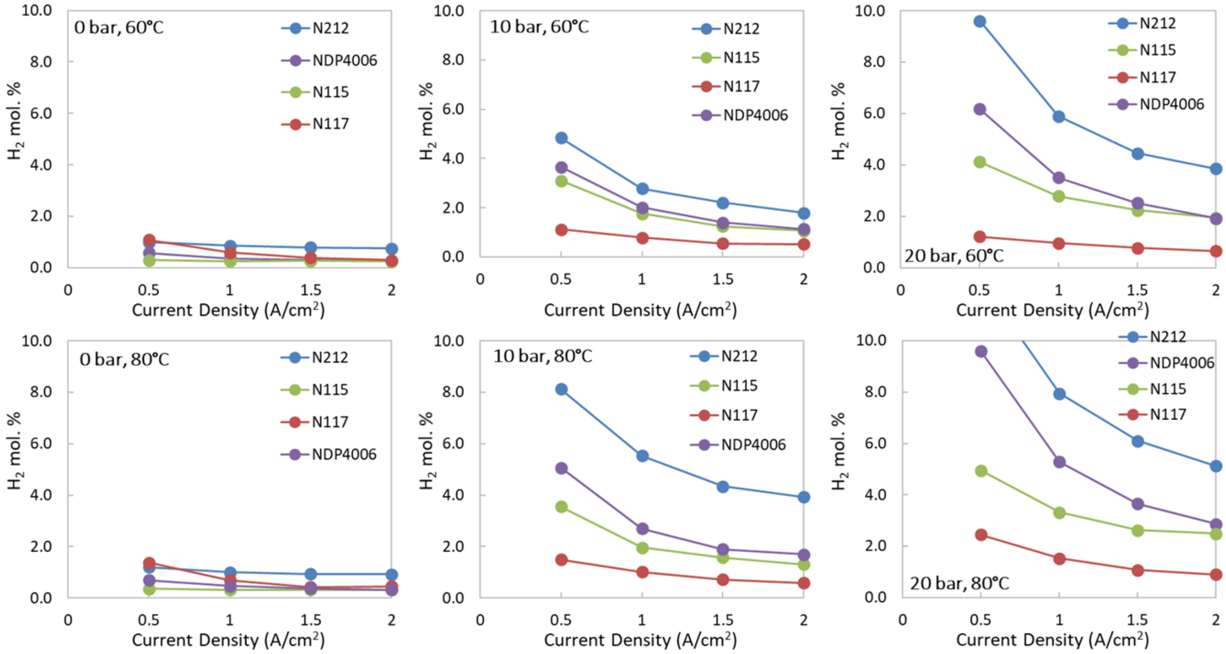

Figure 35. Hydrogen in Oxygen Content for Baseline Membranes between 60-80°C and 0-20 bar H_2 Backpressure.

The combined crossover and polarization data for N117 (thickest) and NR212 (thinnest) membranes are analyzed for faradaic (hydrogen) efficiency and energy consumption in Figures 36 and 37. As can be seen in Figure 36, for all conditions, faradaic (hydrogen) efficiency losses, even for the thinnest membrane NR212, are reasonably modest. Only at the highest temperature (80°C), back pressure (30 bar H_2), and lowest current density (0.2 A/cm^2) does any efficiency loss due to hydrogen crossover exceed 10%. When the efficiency data are used to calculate overall energy requirement as a function of current density in Figure 37, the obvious conclusion is that the voltage efficiency gained from lower voltage in a lower resistance/thinner membrane far exceeds the negative contribution of gas crossover. For current densities 0.5 A/cm^2 and above, the energy needed to generate a kilogram of hydrogen is larger for N117 than NR212. As NR212 has higher crossover and poorer polarization than pilot scale GRC membranes in this project, the conclusion would be even stronger for pilot scale membranes and this calculation was not explicitly repeated for further membranes.

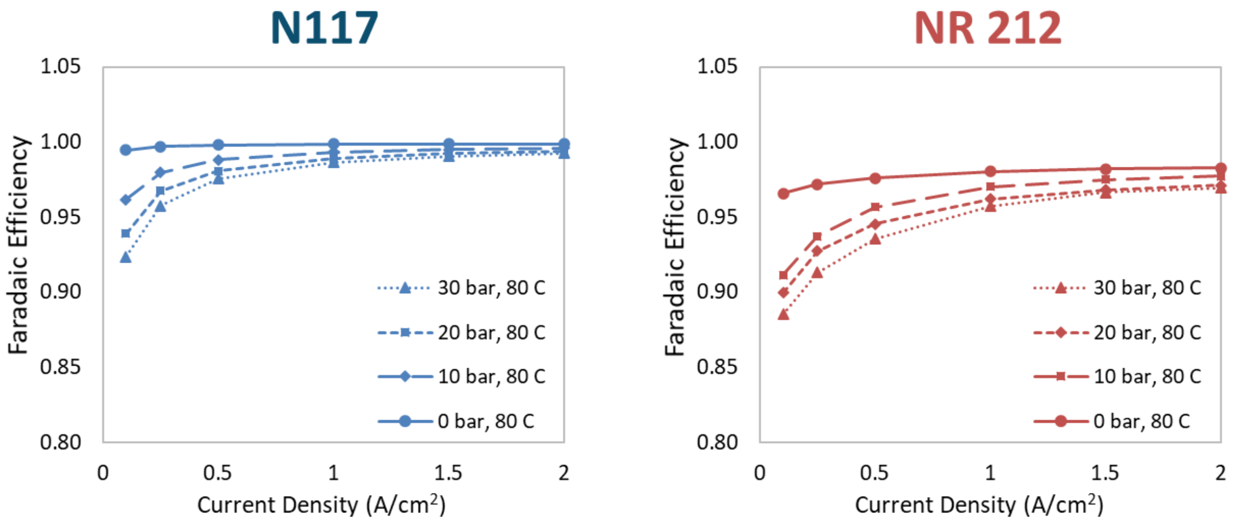

Figure 36. Faradaic (hydrogen) efficiency calculated from equation 1 for N117 and NR212 membranes.

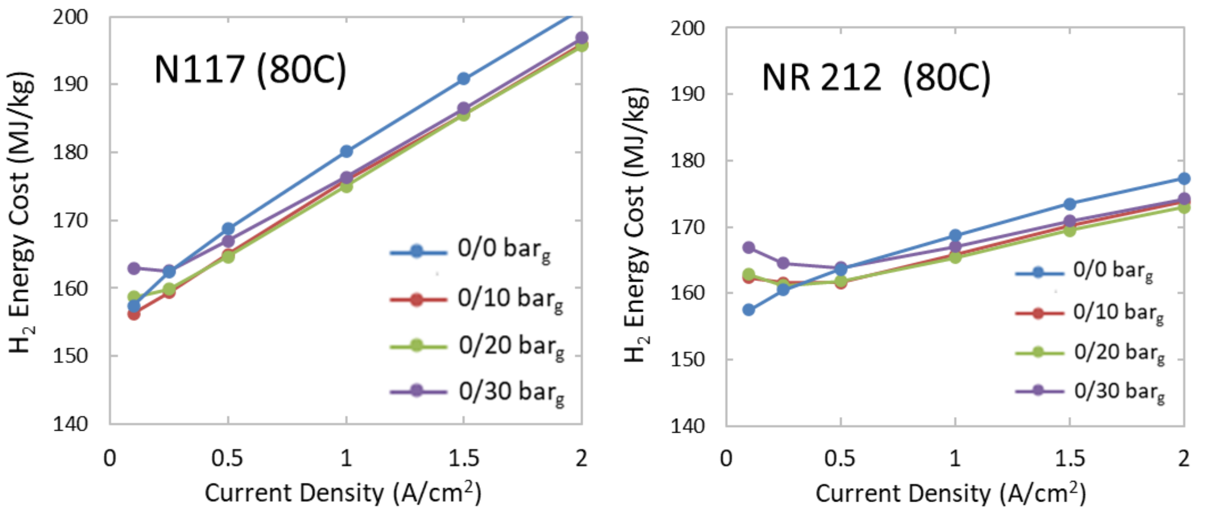

Figure 37. Energy consumption to make hydrogen as a function of current density for N117 and NR212 membranes.

A summary of the most relevant/instructive data regarding experimental GRC-containing membranes will be provided below (please see AMR presentations for further data). For example, four membranes with a varying loading of GRC were tested at NREL (including a control NR212 with 0 GRC). The highest loaded membrane contained <0.075 mg/cm^2 of GRC, and the low-medium-high membranes contained roughly 1x-2x-3x the amount of GRC relative to one another. The influence of loading is quantified in Figure 38. Even a small amount of GRC is effective to reduce effective crossover from baseline, but the highest amount is required to ensure <4% H_2 in O_2 for all current densities at 80°C and 30 bar H2 pressure. It should be noted that even the “high” loaded sample is below targeted GRC loadings (<0.075 mg/cm^2, see Table 1), which is a small fraction of the total electrode PGM loading from Table 9. These data, along with other membranes from AMR presentations, satisfy **Milestone M6:** *Manufacture and evaluate series (minimum 5 different samples) of membranes with different thicknesses and GRC layer compositions to determine effect of GRC placement/loading on H2 in O2 content targeting <2% H2 in O2 for all current densities between 0.5 and 2 A/cm2.*

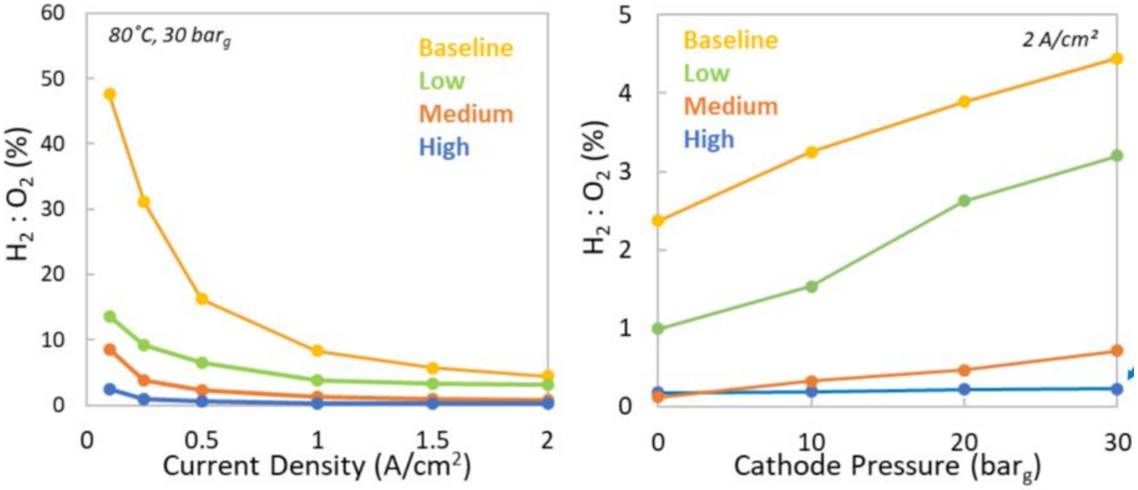

Figure 38. GRC effective crossover reduction as a function of GRC content.

A summary of crossover results from lab scale and pilot scale membranes is presented in Figure 39 below. The two lab scale membranes are included to highlight the range of possibilities in terms of GRC performance. One membrane is capable of mitigating the hydrogen crossover across all current densities, while another is not capable of meeting the lower flammability limit target at low current densities. These data are best observed at high cathodic backpressure, as this high crossover load best resolves poor GRC configurations from successful ones. Pilot scale 1 membrane is shown as well, indicating that the best lab scale GRC strategy from early work in this project was able to be successfully manufactured on a roll-to-roll manufacturing line at Chemours. Lab Scale membrane 1 fulfills the requirements found in **Go/No-Go G1**: *A ≤50 µm thick PFSA-based membrane with gas recombination catalyst layer (GRC PGM maximum loading of 0.1 mg/cm2) demonstrates at least 50% reduction in H2 in O2 (outlet) content (maximum of 2% H2 in O2 for all current densities between 0.5 and 2 A/cm2) compared to membrane with equivalent thickness without GRC layer. Membrane resistance must be <0.07 Ω-cm2 and current density must reach 2 A/cm2 at <1.9V, with all targets to be met in a PEMWE MEA at 60°C and with a differential pressure of 1-10 bar.* Pilot scale Membrane 1 meets **Milestone M7**: *Achieve H_2 in O_2 content of <2% for all current densities between 0.5 and 2 A/cm2 for a membrane with a GRC layer as a function of hydrogen back pressure from 10-30 bar in a PEMWE MEA at 60°C.*

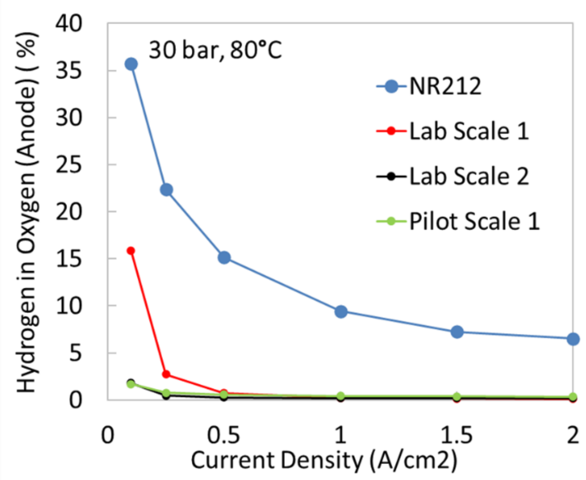

Figure 39. Measured H_2:O_2 ratio for lab and pilot scale GRC-containing MEAs at various current densities (0-2 A cm^{-2}), temperatures (60-80°C), and backpressures (0-30 barg, cathode).

Table 5 described the pilot membrane runs intended to produce optimized candidate membranes for final composition down-selection. The crossover observed in these membranes is displayed below in Figure 40. Pilot membrane 3, whose electrochemical performance exceeded DOE targets for 1.8 V at 3 A/cm^2, mitigates crossover below 10% of the lower flammability limit for hydrogen in oxygen. Compared to NR212, the crossover has been reduced by greater than a factor of 50x (each membrane is 50 µm). Pilot membrane 3 can be understood as the fulfillment of **Milestone M10**: *Optimize GRC and radical scavenger additives content with a Pt loading of <0.05 mg/cm2 for use in large scale R2R manufacturing of <50 µm membrane.* It should be noted that the values below represent crossover data for membranes exposed to a PEMWE environment for 24 hours.

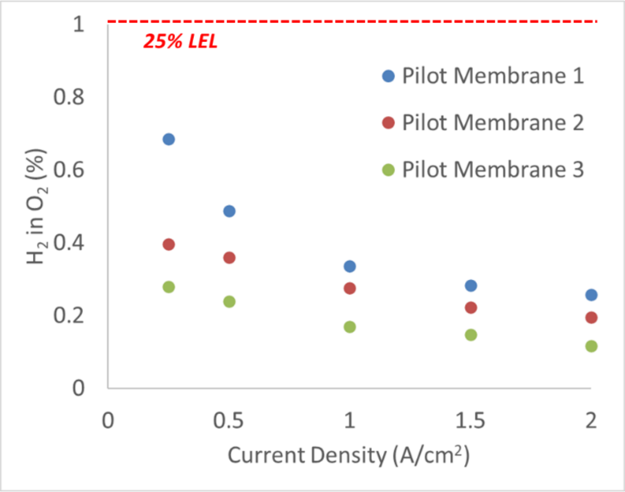

Figure 40. Hydrogen in oxygen content for three pilot line membranes made by Chemours and evaluated at NREL. Testing was done at 80°C and 30 bar H_2 backpressure.

A critical component of membrane success is the durability of the crossover mitigation over time. In order to evaluate the consistency of the crossover mitigation scheme, pilot scale membrane 1 was held at constant current (2 A/cm^2) at 80°C for 500 hours. Crossover was periodically measured from 0.1-2 A/cm^2 current density, with results presented in Figure 41. Particularly for low current densities, a slow but constant uptick in effective gas crossover is noted over the 500-hour duration.

While the mitigation at higher current does not increase as dramatically, a small but constant increase is noted even for 2.0 A/cm^2 current density. Figure 42 plots the crossover at 2 A/cm^2 as a function of time for membranes 22-1x (pilot scale membrane 1) and 30-1x (pilot scale 2). While the improvement from figure 40 is replicated in the overall gas crossover between membranes 1 and 2, the slow increasing trend of increased effective gas crossover is replicated in both MEAs.

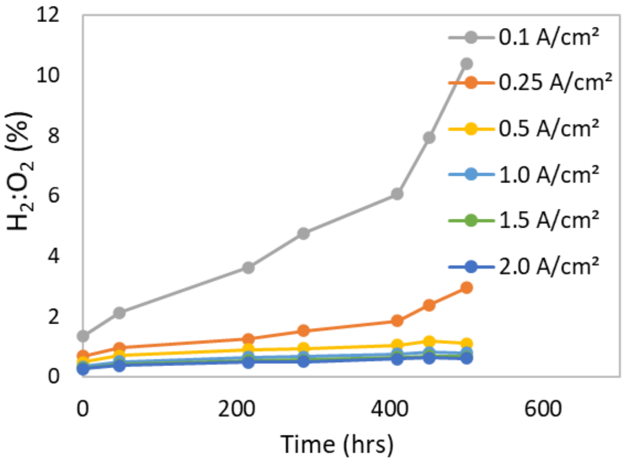

Figure 41. Hydrogen crossover for 22-1X Membrane as a function of time at several current densities.

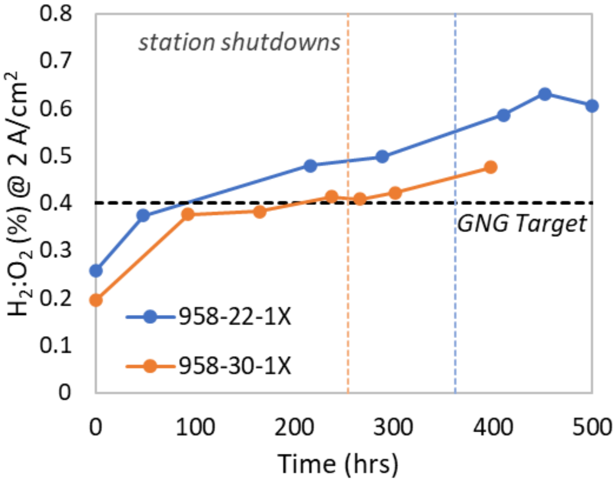

Figure 42. Hydrogen crossover for 22-1x and 30-1x membranes as a function of time at 2 A/cm^2. Go/No-Go (G2) target included as dashed line.

The data in Figures 40 and 42 do not completely meet the target of **Go/No-Go 2 (G2):** *Reinforced roll-to-roll dispersion cast membrane with GRC (<0.075 mg PGM/cm2) and radical scavenging additives demonstrates a H2 in O2 content of <2% for all current densities between 0.5 and 2 A/cm2 where membrane thickness is ≤ 50 μm, membrane resistance is < 0.05 Ω-cm2, and hydrogen backpressure is 30 bar. Voltage in an MEA at 2 A/cm2 must be < 1.9 V and membrane resistance/gas crossover must remain <0.4% H2 in O2 after 500 hr of continuous operation at 60°C and differential pressure of 30 bar.* All targets are met with the exception of "<0.4% H_2 in O_2 after 500 hours." While membranes with improved crossover were manufactured (pilot membrane 3), test station bandwidth limitations did not enable further testing for hundreds of hours at high backpressure. The 0.4% H_2 in O_2 target is 10% of the lower flammability limit threshold, which is an aggressive target that represents the endpoint commercial goal for these membranes. After discussion with DOE Project Management, it was agreed that this target was aspirational and overly challenging for an intermediate progress metric intended to demonstrate progress toward the ultimate membrane goal. Since each pilot scale membrane neared the target by demonstrating ~0.6% and 0.45% H_2 in O_2 at 2 A/cm^2 after 500 and 400 hours, respectively, the project was allowed to proceed into Budget Period 3.

It should be noted that 500 hours is not an extraordinary amount of time to test a membrane, and the changes could represent an expected "break-in" process of the MEA over time. However, assuming the effect would persist beyond 500 hours, two overall hypotheses for this degradation in crossover mitigation include (1) reduction in effectiveness of the GRC over time (i.e., migration within or out of MEA, particle size growth, poisoning, etc.) and (2) overall membrane morphological changes due to cell hardware. The first hypothesis cannot be ruled out at this time. As presented in Tables 7 and 8, migration has not been observed for GRC in a pilot membrane in the ex-situ cell hardware at LANL. However, it is difficult to measure in-situ migration in an MEA experiment due to the obfuscating presence of PGM catalysts in an MEA and the finding could not be confirmed for these membranes. It has also been proposed that the anode catalyst material, Ir, which slowly undergoes dissolution over time, could be transported through the membrane and deposits onto the GRC surface, which could reduce its activity. These hypotheses could be verified in the future with more advanced characterization techniques but were not pursued in the course of this project.

However, there is a significant change observed in the topography of the membrane/electrode surface facing the anode. A cross-section SEM of the MEA employing 22-1x membrane after 500 hours of operation – representing an "end of life" MEA in this project – is presented below in Figure 43. Membrane deformation, associated with penetration of ionomer into the pores of the titanium porous transport layer (PTL) material, is apparent in the SEM micrograph. As the GRC material is preferentially located within the membrane adjacent/near to the anode electrode, this local topography change could reduce effective GRC layer thickness in some areas and possibly neutralize/render ineffective the GRC contained in the protruding ionomer.

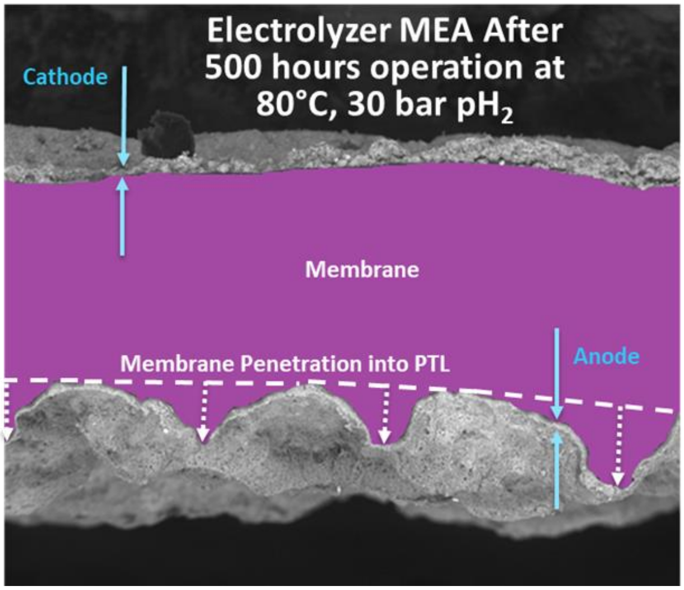

Figure 43. SEM images of an MEA after 500 hours of operation at 80C and 30 bar hydrogen backpressure.

The topographical change between an MEA subjected to 24 hours of galvanostatic hold (not pictured) is compared to that after 500 hours in Figure 44. The average topographical change, measured by distance from tip of individual protrusion from baseline for a series of ionomer features, is more strongly pronounced at 500 hours by a factor of 2. This result suggests that the morphological changes manifest more strongly over time, which could explain (at least in part) the diminishing effect of crossover mitigation observed.

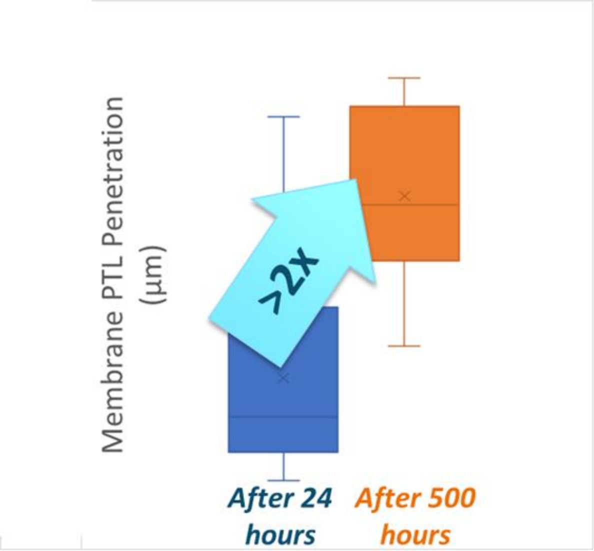

Figure 44. Change in local ionomer penetration depth in a 22-1X membrane over 24 hours and 500 hours.

Subsequent “durability” testing (galvanostatic holds with periodic crossover measurement) were only possible in an ambient pressure configuration. The results for pilot membrane 3 over 1000 hours is presented in Figure 45. As has been noted in the previous membrane evaluations in Figure 43, an increase in effective gas crossover is noted for all current densities. However, by the end of the 1000 hour test, it appears that the trend is starting to level off. This result could suggest that the membrane is experiencing an extended break-in period after which the gas crossover mitigation would stabilize. It also suggests that membrane evaluation for crossover mitigation should account for changes over the first few hundred hours rather than rely only on “beginning of life” data.

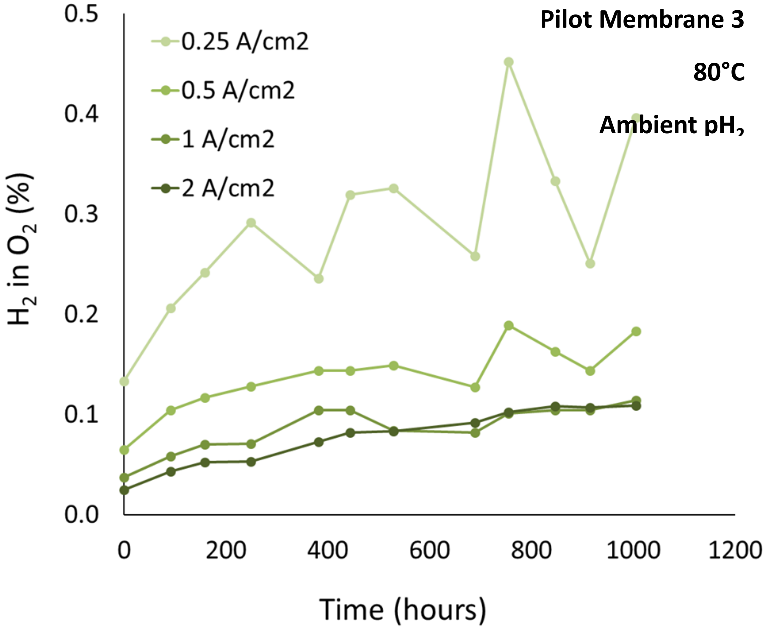

Figure 45. Pilot Membrane 3 evaluated in FuGeMEA configuration at 2 A/cm^2 for 1000 hours, where crossover is periodically measured.

Pilot Membrane 3 satisfies the bulk of **Milestone M12**: *Demonstrate prototype manufacturing of > 100 linear meters of down-selected membrane design on Chemours’ R2R manufacturing line with < 0.05 Ω-cm2 membrane resistance, < 1% H2 in O2 content for all current densities in an MEA, > 10 mg/L Fe(III) tolerance, with additive nanoparticle mobility of < 2.1x10-8 m2/Vs, maintaining > 50% concentration in the membrane and improved lifetime after defined duty cycle/AST, with capacity to produce membranes at costs/rates comparable to Nafion™ XL*. The metric around prototype manufacturing was aligned with DOE Project Management to be understood as “able to be manufactured” rather than specifically manufacturing membrane only to meet the milestone language. As discussed earlier,

5. Membrane and Crossover Modeling

Another node partner in this project was Lawrence Berkeley National Lab (LBNL), whose work in modeling and creep testing is summarized below. The means by which product gas transports away from the catalyst undergirds the mathematical foundation of a PEMWE cell model and is summarized below in Figure 46 with a cartoon depicting the different assumptions. Correctly modeling product gas is a critical foundation to understanding how GRC catalysts can mitigate it in a membrane application.

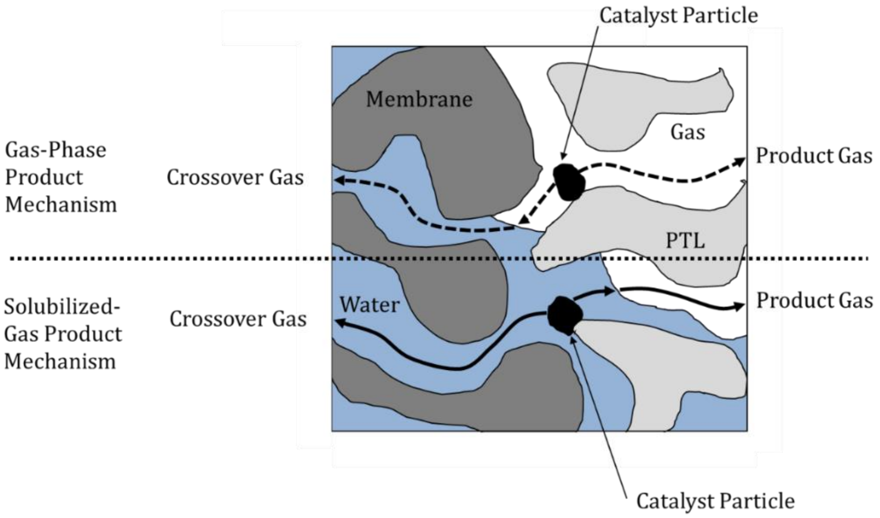

Figure 46. Illustration showing gas-phase and solubilized-gas product mechanisms for hydrogen/oxygen transport in a PEMWE electrode.

The anodic hydrogen concentration equations predicted by either model scheme are summarized below in Figure 47. The critical difference between them is that gas phase product model predicts that hydrogen approaches an asymptote of 0 at high current density (high oxygen content), where solubilized-gas product model approaches a non-zero asymptote. In figure 48, comparing the model to experimental data in three different cell designs suggests that the hydrogen crossover results in non-zero gas crossover as a function of current density, which is best predicted by solubilized-gas phase product.

- Gas-phase product
    - $y_i = \frac{N_i}{\sum_j N_j}$
        - When current is small $y_i \rightarrow 1$
    - Propose correction for low current $y_{i,\text{obs}} = \frac{y_{i,0}\, y_i}{y_{i,0} + y_i}$
- Solubilized-Gas product
    - $y_i = \frac{R_{\text{sol},i}}{\sum_j R_{\text{sol},j} + R_{\text{rxn}}}$

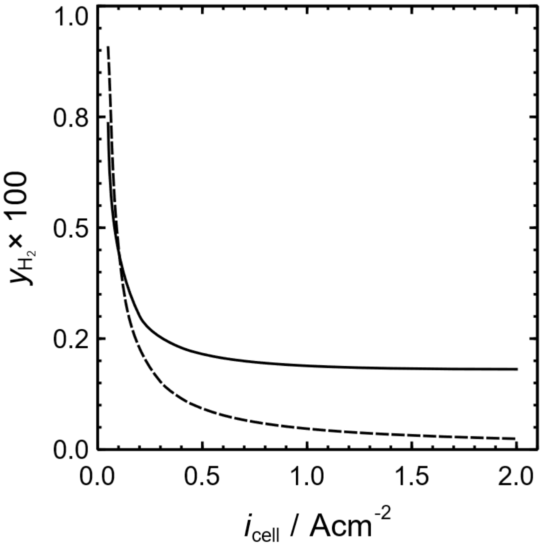

Figure 47. Modeled hydrogen concentration at the anode as a function of cell current density

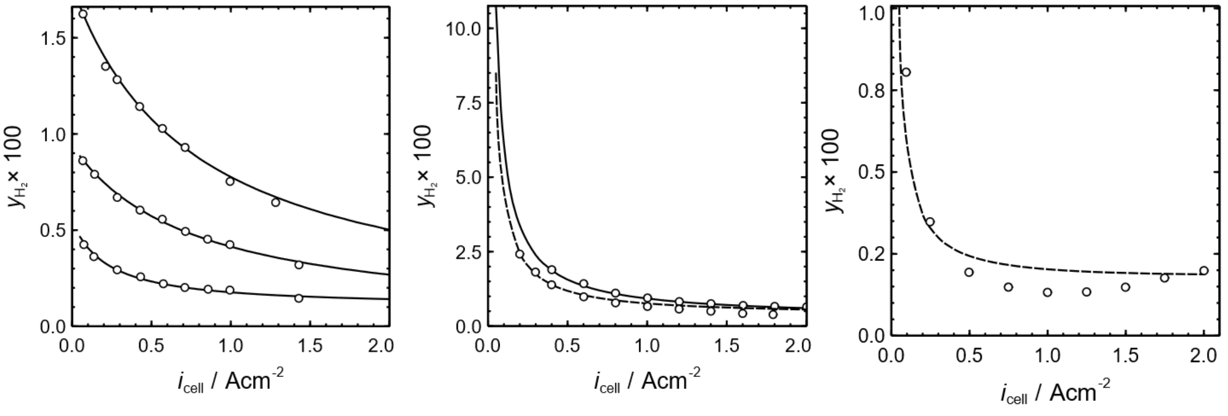

Milliet et al., 2015 Schalenbach et al., 2013 Klose et al., 2019

Figure 48. Model predictions in three separate systems compared to experimental data for hydrogen content in oxygen effluent stream.

Initial polarization and hydrogen crossover data were successfully fitted to the developed PEMWE model and shown in Figure 49 below.

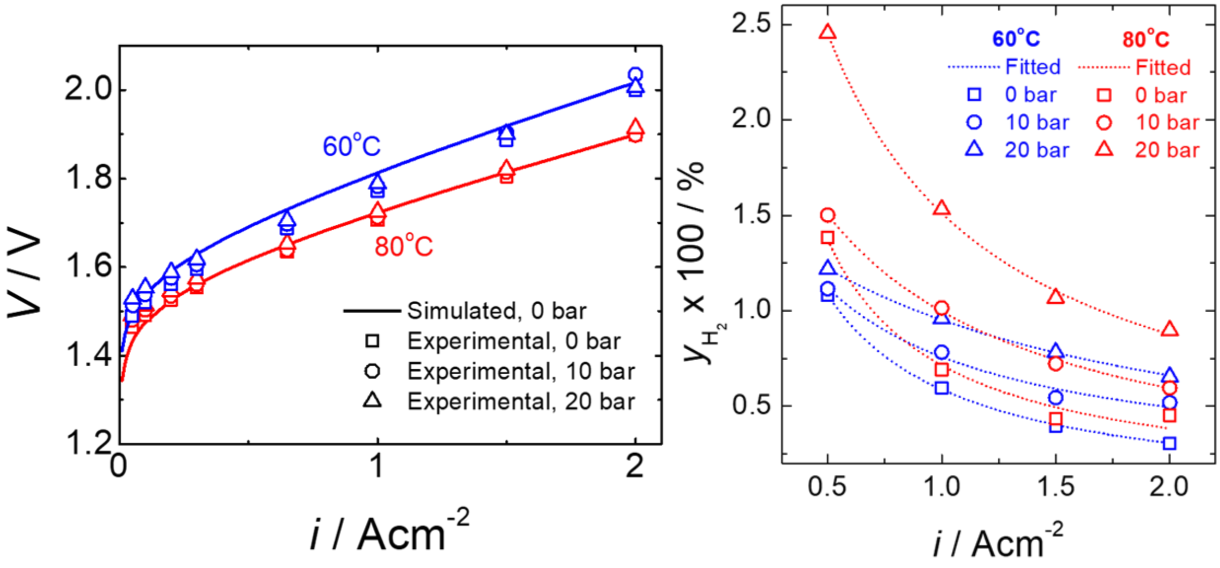

Figure 49. Model-fit to NREL polarization data and hydrogen crossover data at 60C and 80C for N117 membranes

In Figure 50, the crossover data is leveraged with the developed mechanistic model to project the dissolved gas concentrations for oxygen and hydrogen within a 50 µm thick membrane in a balanced pressure environment (1 bar) or differential pressure (pH2 = 15 bar). For a scenario with balanced pressure, the dissolved gas concentration is closer to the cathode, but for a differential pressure environment, the concentrations are equal far closer to the anode. This work confirms the idea that GRC within a membrane must be sided toward the anode in order to most effectively recombine hydrogen/oxygen in an industrially relevant application.

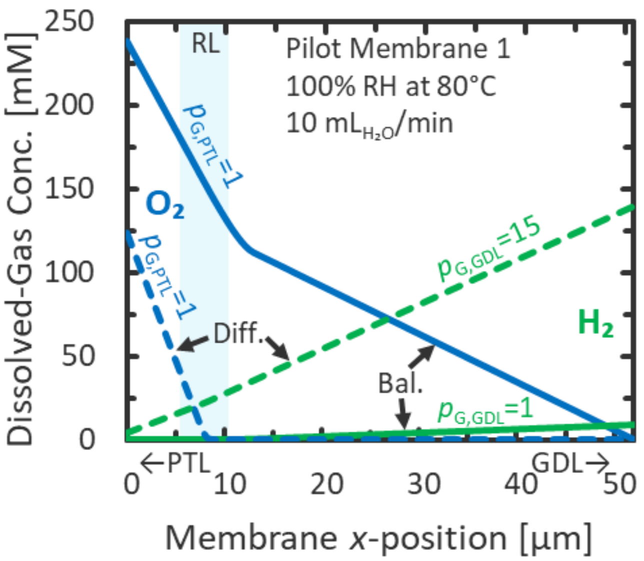

Figure 50. Dissolved-gas conc. of O_2 (blue) and H_2 (green) influenced by operating pressures and RL. Balanced (solid) and differential (dashed) with gas pressures (p_G) in bar.

Significant Accomplishments and Conclusions:

The work in this project represents exciting promise toward a step change in efficiency for clean, low-cost hydrogen production. Membranes have been manufactured with a significant reduction in proton transport resistance that enables a stack efficiency of 72% versus 60% for baseline membranes. A more efficient stack implies less electricity used to generate a given mass of hydrogen, which is directly relevant toward the DOE's Hydrogen Shot target of $1/kg H_2. The GRC concept has proved very effective, with a 50x reduction in gas crossover observed compared to GRC-free membranes. Developed capabilities have proven invaluable in the determination of membrane crossover, where ex-situ and operando cell testing at 30 bar differential pressure were implemented and operated for hundreds of hours. However, the ultimate test of membrane success would be for the GRC mitigation to have been proven consistent for thousands of hours. Even with limited testing bandwidth and relevant conditions, it is likely that more work will be required to ensure a membrane/GRC strategy is compatible with stable operation in a PEMWE environment.

There are several strategies to explore that merit further study to improve durability. First, new PTL materials with "microporous layer" (MPL) analogues, as in modern fuel cell gas diffusion layers, are in development and could reduce the open pore space available for membrane to penetrate. These can be integrated into advanced cell designs that allow exchangeable components and evaluated over time. If the topographical change must be accepted as a consequence of high temperature and high backpressure MEA operation, other solutions can be explored to mitigate it. For example, the effect of polymer equivalent weight and molecular weight on the penetration of membrane into PTL pores has not been studied, and this project could influence/suggest future work on this topic. Other advanced reinforcements could make membranes more/less susceptible to this effect as well. Using this finding could also influence membrane design to make GRC layers more resilient to deformation.

Also, an unresolved discrepancy between ex-situ and operando membrane crossover was found within this project's work. The novelty of operating cell hardware at pressures around 30 bar represented a significant learning curve that was ultimately not concluded within this project. It should be noted that inherent differences in GRC behavior during operando MEA testing versus ex-situ, electrode free simple crossover experiments cannot be ruled out. Further work in this area should build upon this finding to understand better the relationship between current, voltage, and GRC behavior.

Path Forward: Future R&D in this subject area requires proving out product concepts in progressively larger scale test platforms for hundreds to thousands of hours. Test cell hardware and subcomponents such as PTLs much be engineered to facilitate thin membrane acceptance. It is possible that the thin membrane approach may not enable tens of thousands of hours of device lifetime – specific mechanical property testing to probe failure mechanisms could elucidate this risk. Partnership with established OEMs in this space with test capability/bandwidth at high cathodic backpressures would be critical to progress. Given the limited results in the 500 hour testing platform, it is unlikely that the specific candidate (Pilot Membrane 3, for example) would be commercialized as-is, but it should represent significant progress toward the commercialization of high performance, durable, domestic membranes for PEMWE applications.

Products:

1. I01F-1249 (Invited) Progress in Nafion™ Membrane Development for Proton Exchange Membrane Water Electrolyzers, R. Gebhardt, D. Manion, B. Wright (The Chemours Company), J. A. Wrubel (National Renewable Energy Laboratory), C. E. Van Pelt (Los Alamos National Laboratory), A. Dizon (Lawrence Berkeley National Laboratory), J. Zack (National Renewable Energy Laboratory), A. Z. Weber (Lawrence Berkeley National Laboratory), R. L. Borup (Los Alamos National Laboratory), G. Bender (National Renewable Energy Laboratory), S. Komini Babu (Los Alamos National Laboratory), and A. M. Park (The Chemours Company)

2. I01F-1247 In-Operando Measurement of Hydrogen Crossover in Proton Exchange Membrane Electrolysis Cells at Differential Pressures

J. A. Wrubel, J. Zack (National Renewable Energy Laboratory), A. Dizon, A. Z. Weber (Lawrence Berkeley National Laboratory), A. M. Park (The Chemours Company), and G. Bender (National Renewable Energy Laboratory)

3. Wrubel, J.A., Milleville, C., Klein, E.C., Zack, J., Park, A.M., and Bender, G., "Estimating Hydrogen Energy Cost of Proton Exchange Membrane Electrolysis Cells

using Rapid Operando Hydrogen Crossover Analysis", International Journal of Hydrogen Energy.

4. Wrubel, J.A., Kowal, A., Park, A.M., and Bender, G. H2 Crossover in High Pressure PEM Electrolysis. 242nd ECS Meeting Atlanta, GA 2022.

5. Khedekar, K, Van Pelt, C.E., Gebhardt, R., Zenyuk, I., Bender, G., Mukundan, R., Park, A.M., Borup, R., Babu, S.K. Understanding Gas Permeation during High Pressure Operation of PEM Water Electrolyzers. 242nd ECS Meeting Atlanta, GA 2022.

6. Xiang Lyu, Jayson Foster, Robin Rice, Elliot Padgett, Erin B. Creel, Jianlin Li, Haoran Yu, David A. Cullen, Nancy N. Kariuki, Jae Hyung Park, Deborah J. Myers, Scott Mauger, Guido Bender, Svitlana Pylypenko, Alexey Serov. Aging gracefully? Investigating iridium oxide ink's impact on microstructure, catalyst/ionomer interface, and PEMWE performance. J. of Power Sources Volume 581, 15 October 2023, 233503

7. Wang, C et al., Proton Exchange Membrane (PEM) Water Electrolysis: Cell-Level Considerations for Gigawatt-Scale Deployment. Chem. Rev. 2025, 125, 3, 1257–1302.

Project Team and Roles: **Chemours**: Andrew Park - PI and Project Lead, Ryan Gebhardt, Rebekah Wright, Sam Bartuska, David Prugh, George Brown, Meghan Vander Woude, Austin Plymill – Staff Scientist Participants. **LANL**: Rod Borup, Siddharth Komini Babu – Co-PI(s), Evan Van Pelt – Student, Kaustubh Khedekar – Postdoc. **NREL**: Guido Bender – Node PI, Jake Wrubel – Staff Scientist, Corey Schaeffer, Jason Zack, Ellis Klein – Staff Scientists, Andrea Kowal – Student. **LBNL**: Adam Weber, Ahmet Kusoglu – node PIs, Arthur Dizon – Staff Scientist.

References:

(1) The Chemours Company. Product Bulletin P-12: NafionTM N115, N117, N1110.

(2) Su, H.; Bladergroen, B. J.; Pasupathi, S.; Linkov, V.; Ji, S. Performance Investigation of Membrane Electrode Assemblies for Hydrogen Production by Solid Polymer Electrolyte Water Electrolysis. *Int J Electrochem Sci* **2012**, *7* (5), 4223–4234. https://doi.org/https://doi.org/10.1016/S1452-3981(23)19533-2.

(3) Bessarabov, D. (Invited) Membranes with Recombination Catalyst for Hydrogen Crossover Reduction: Water Electrolysis. *ECS Trans* **2018**, *85* (11), 17. https://doi.org/10.1149/08511.0017ecst.

(4) Hamdan, M. Electrochemical Compression. In *Annual Merit Review Meeting*; 2018.

(5) Gubler, L.; Dockheer, S. M.; Koppenol, W. H. Radical (HO • , H • and HOO •) Formation and Ionomer Degradation in Polymer Electrolyte Fuel Cells. *J Electrochem Soc* **2011**, *158* (7), B755–B769. https://doi.org/10.1149/1.3581040.

(6) Baker, A. M.; Babu, S. K.; Mukundan, R.; Advani, S. G.; Prasad, A. K.; Spernjak, D.; Borup, R. L. Cerium Ion Mobility and Diffusivity Rates in Perfluorosulfonic Acid Membranes Measured via Hydrogen Pump Operation. *J Electrochem Soc* **2017**, *164* (12), F1272–F1278. https://doi.org/10.1149/2.1221712jes.

(7) Abbas, D.; Martin, A.; Trinke, P.; Bierling, M.; Bensmann, B.; Thiele, S.; Hanke-Rauschenbach, R.; Böhm, T. Effect of Recombination Catalyst Loading in PEMWE Membranes on Anodic Hydrogen Content Reduction. *J Electrochem Soc* **2022**, *169* (12), 124514. https://doi.org/10.1149/1945-7111/aca6a0.

(8) Klose, C.; Trinke, P.; Böhm, T.; Bensmann, B.; Vierrath, S.; Hanke-Rauschenbach, R.; Thiele, S. Membrane Interlayer with Pt Recombination Particles for Reduction of the Anodic Hydrogen Content in PEM Water Electrolysis. *J Electrochem Soc* **2018**, *165* (16), F1271–F1277. https://doi.org/10.1149/2.1241814jes.

(9) Parimuha, M. R.; Young, J. L.; Lee, J. K.; Yilmaz, A.; Diaz-Abad, S.; Gawas, R.; Schuler, T.; Komini Babu, S.; Bender, G. Proton Exchange Membrane Electrolysis Benchmarking: Identifying and Removing Sources of Variation in Test Stations, Hardware, and Membrane Electrode Assembly Fabrication. *Int J Hydrogen Energy* **2025**, *114*, 486–496. https://doi.org/10.1016/J.IJHYDENE.2025.02.443.